The Canadian Mineralogist
Vol. 37, pp. 277-296 (1999)

HARKERITE AND ASSOCIATED MINERALS IN MARBLE AND SKARN FROM CRESTMORE QUARRY, RIVERSIDE COUNTY, CALIFORNIA AND CASCADE SLIDE, ADIRONDACK MOUNTAINS, NEW YORK

EDWARD S. GREW[1] AND MARTIN G. YATES

Department of Geological Sciences, University of Maine, Orono, Maine 04469, U.S.A.

PAUL M. ADAMS

The Aerospace Corporation, P. O. Box 92957, Mail Station M2-250, Los Angeles, California 90009, U.S.A.

RUTH KIRKBY

P.O. Box 12455, Scottsdale, Arizona 85267, U.S.A.

MICHAEL WIEDENBECK[2]

Advanced Materials Laboratory, University of New Mexico, Albuquerque, New Mexico 87106, U.S.A.

ABSTRACT

Of two newly described North American localities for harkerite, ~ $Ca_{48}\,Mg_{16}\,[AlSi_4O_{15}(OH)]_4\,(BO_3)_{16}\,(CO_3)_{16}\,(H_2O,HCl)_2$, the high-temperature, low-pressure contact aureole in the Crestmore quarry is typical for this mineral, whereas the deep-seated Cascade Slide xenolith in anorthosite is unique. Critical assemblages are harkerite + forsterite + clintonite ± spinel (Crestmore marble), harkerite + monticellite ± forsterite + spinel and harkerite + clinopyroxene + monticellite (Cascade Slide marble), and harkerite + vesuvianite + monticellite + clintonite (Crestmore skarn). The sequence of crystallization at both localities is first monticellite, then forsterite, and lastly, harkerite; at Crestmore, clintonite formed after forsterite and spinel. Variations in SiO_2, Al_2O_3 and B_2O_3 in harkerite approximately fit the substitution $(BO_3)_4 \rightleftharpoons Al_{0.75}Si_{4.25}O_{15.25}(OH)_{0.75}$. The distribution of Fe^{2+} and Mg among the minerals is regular, and the ratio Fe^{2+}/Mg increases in the sequence forsterite < harkerite < spinel < monticellite << magnetite. This regularity is consistent with most Fe being Fe^{2+} in harkerite and with approach to chemical equilibrium between harkerite and associated minerals. At Crestmore, the harkerite formed at close to peak temperature, when fluid introduced Al into the aureole. The boron was presumably introduced by this fluid at Crestmore, whereas it could have been present in the precursors to the harkerite-bearing rocks at Cascade Slide. The Cascade Slide harkerite probably formed at high temperature and low pressure in a marble xenolith entrapped in anorthosite at a high level in the crust, and re-equilibrated during granulite-facies metamorphism. Harkerite was stable at the 7–8 kbar pressure estimated for this metamorphism, but only because of the near-absence of a fluid phase.

Keywords: harkerite, monticellite, forsterite, spinel, contact aureole, ion microprobe, Adirondack Mountains, New York, Crestmore quarry, California.

SOMMAIRE

Des deux nouveaux indices de harkerite, ~ $Ca_{48}\,Mg_{16}\,[AlSi_4O_{15}(OH)]_4\,(BO_3)_{16}\,(CO_3)_{16}\,(H_2O,HCl)_2$, situés en Amérique du Nord, c'est l'auréole de contact à température élevée et faible pression exploitée dans la carrière de Crestmore, en Californie, qui présente le milieu de formation typique de ce minéral. En revanche, le xénolithe d'origine profonde découvert dans une anorthosite à Cascade Slide, dans la chaîne Adirondack, New York, semble unique. Les assemblages critiques sont: harkerite + forstérite + clintonite ± spinelle (marbre de Crestmore), harkerite + monticellite ± forstérite + spinelle et harkerite + clinopyroxène + monticellite (marbre de Cascade Slide), et harkerite + vésuvianite + monticellite + clintonite (skarn de Crestmore). La séquence de cristallisation aux deux endroits est d'abord monticellite, ensuite forstérite et, finalement, harkerite; à Crestmore, la clintonite s'est formée après la forstérite et le spinelle. Dans la harkerite, les variations en SiO_2, Al_2O_3 et B_2O_3 respectent *grosso modo* la substitution $(BO_3)_4 \rightleftharpoons Al_{0.75}Si_{4.25}O_{15.25}(OH)_{0.75}$. La distribution de Fe^{2+} et Mg parmi les minéraux est régulière, et le rapport

---

[1] *E-mail address*: esgrew@maine.edu

[2] Present address: ProjektBereich 4.2, GeoForschungsZentrum Potsdam, D-14473 Potsdam, Germany.

Fe^{2+}/Mg augmente dans la séquence forstérite < harkerite < spinelle < monticellite << magnétite. Cette régularité concorde avec l'hypothèse voulant que le Fe est surtout à l'état ferreux dans la harkerite, et que celle-ci se rapproche de l'équilibre avec les minéraux associés. A Crestmore, la harkerite s'est formée près de la température maximale du métamorphisme, quand la phase fluide a introduit l'aluminium dans la zone de contact. Le bore a probablement aussi été introduit par cette phase fluide à Crestmore, tandis qu'à Cascade Slide, il était peut-être présent dans le précurseur des roches à harkerite. A cet endroit, la harkerite s'est probablement formée à température élevée et à faible pression dans un xénolithe de marbre piégé dans une anorthosite à faible profondeur dans la croûte, et ré-équilibrée au cours du métamorphisme dans le faciès granulite. La harkerite est restée stable dans l'intervalle de pression de 7–8 kbar que l'on préconise pour cet épisode de métamorphisme, mais seulement à cause de l'absence presque totale d'une phase fluide.

(Traduit par la Rédaction)

Mots-clés: harkerite, monticellite, forstérite, spinelle, auréole de contact, microsonde ionique, chaîne des Adirondack, New York, carrière de Crestmore, Californie.

INTRODUCTION

Harkerite, a complex Ca–Mg carbonate–borate–silicate with an approximate formula $Ca_{48} Mg_{16} [AlSi_4O_{15} (OH)]_4 (BO_3)_{16} (CO_3)_{16} (H_2O,HCl)_2$ (Giuseppetti *et al.* 1977), is typically found in calcareous skarns and other rocks rich in Ca formed at low pressures and high temperatures; thirteen localities have been reported (*e.g.*, Tilley 1951, Pertsev 1971, Barbieri *et al.* 1977, Grew 1996). However, harkerite and the related mineral sakhaite are not restricted to such environments, having also been reported from regional greenschist-facies rocks in South Africa (Innes & Chaplin 1986, Dunn *et al.* 1990), amphibolite-facies rocks in Sweden (Holtstam & Langhof 1995), and from granulite-facies rocks at Cascade Slide, New York (Baillieul 1976).

We present here a detailed description of harkerite and associated minerals from Crestmore quarry, California, and Cascade Slide, New York, including the first analytical results obtained on harkerite with the ion probe. Baillieul (1976) reported an X-ray powder pattern and a petrographic description of harkerite from Cascade Slide, whereas only the mineral association has been cited for Crestmore harkerite (Adams and Grew, unpublished data cited in Grew 1996). In addition, we include our petrographic and chemical data on a specimen from the type locality at Skye, U.K.

PETROGRAPHIC DESCRIPTION

Crestmore quarry

Harkerite was found originally in specimens collected in 1979 from vesuvianite-rich skarn at the 910-foot (358 m) level of the quarry (sample 3). In 1992, harkerite was found in blue calcite marble at the 700 foot (276 m) level underground in the mine (samples 1, 2).

The harkerite-bearing portions of the two marble specimens (#1C, 2A, Table 1) consist dominantly of blue calcite in grains typically from 2 mm to nearly 1 cm across. Harkerite forms subequant grains mostly 1–2 mm across in #1C, and irregular, sprawling grains extending over 5 mm in #2A. Fresh harkerite is in part isotropic, in part has low birefringence; some birefringent patches show mosaic extinction and ill-defined twinning. Harkerite encloses clintonite, spinel, calcite and forsterite. Monticellite was found only in #1C as rare inclusions in forsterite (Fig. 1). Forsterite is commonly twinned, locally in pie-shaped segments (Fig. 2), similar to the trillings in forsterite from skarns metasomatized with boron in Polar Yakutiya (Pertsev 1965). In #1, green spinel occurs invariably as irregular grains ≤0.2 mm across enclosed in clintonite (Fig. 3); locally, a few spinel grains are enclosed in forsterite or calcite. In #2A, spinel grains 0.05–0.35 mm across are found in the calcite matrix and in harkerite, as well as in clintonite (Fig. 4). Anhydrite occurs as isolated grains in the calcite matrix (Fig. 1) or in aggregates with clintonite and harkerite (Fig. 4); it was identified by its orthogonal cleavages, high birefringence, and presence of only Ca and S in a scan with the energy-dispersion system (EDS). The single apatite ("wilkeite") grain in #2A contains minor S, Si and Cl (EDS scan). Perovskite occurs sparingly, typically in contact with clintonite (*e.g.*, Fig. 1).

The skarn specimen contains harkerite, large brown crystals of vesuvianite, poikiloblastic wollastonite, white radiating fibers of jennite replacing crystals of another mineral, and blue calcite. However, wollastonite was not found in the thin section cut for the study of harkerite (#3A, Table 1). A small patch of fresh harkerite showing low birefringence and a mosaic texture in polarized light was found in a large mass that is mostly altered. Clintonite with spinel inclusions and monticellite occurs within the vesuvianite matrix. Calcite forms veinlets and clots, and appears to be secondary.

Cascade Slide xenolith

Our specimens were collected in 1995 (#1, 2) and in 1996 (#3, 4, 5, Table 1) from boulders downstream from Baillieul's (1976, Plate 1) locality for the *in situ* harkerite-bearing specimen TM-16 (Table 1). All specimens showed spots of red fluorescence in shortwave UV

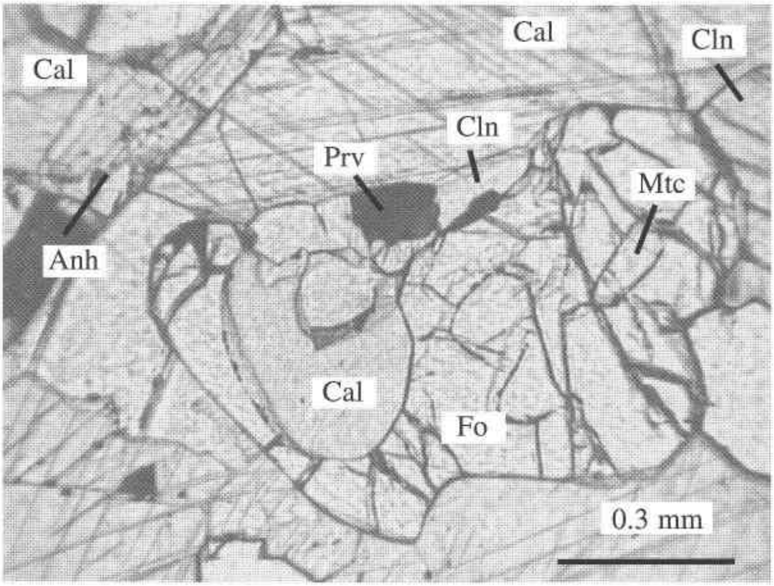

FIG. 1. Photomicrograph of forsterite (Fo) with inclusion of monticellite (Mtc) in Crestmore marble #1C. Perovskite (Prv) is partly surrounded by clintonite (Cln). Anh: anhydrite, Cal: calcite. Compositions of forsterite and monticellite are given in Table 5. Plane-polarized light.

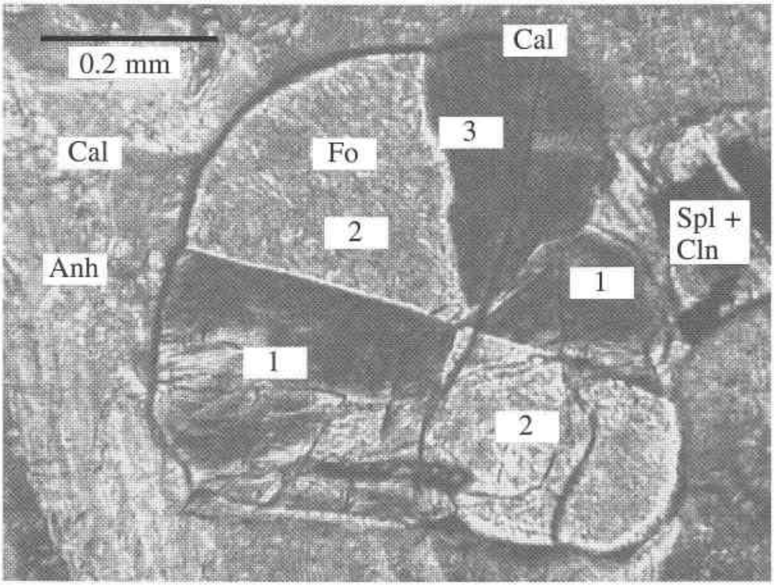

FIG. 2. Photomicrograph of twinned forsterite (Fo) in Crestmore marble #2A. Numbers mark the twin segments, Cal: calcite, Spl: spinel, Cln: clintonite. Crossed nicols.

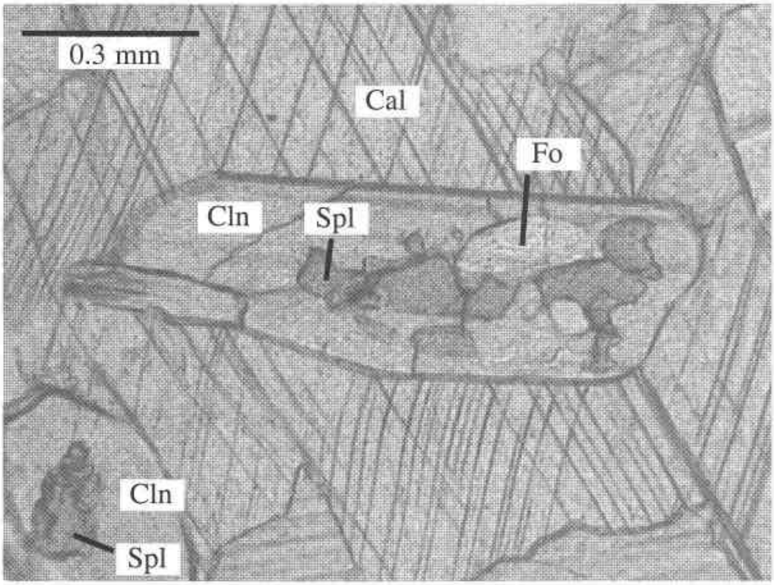

FIG. 3. Photomicrograph of clintonite (Cln) with inclusions of spinel (Spl) and forsterite (Fo) in Crestmore marble #1A (harkerite-free part of sample #1). Cal: calcite. Plane-polarized light.

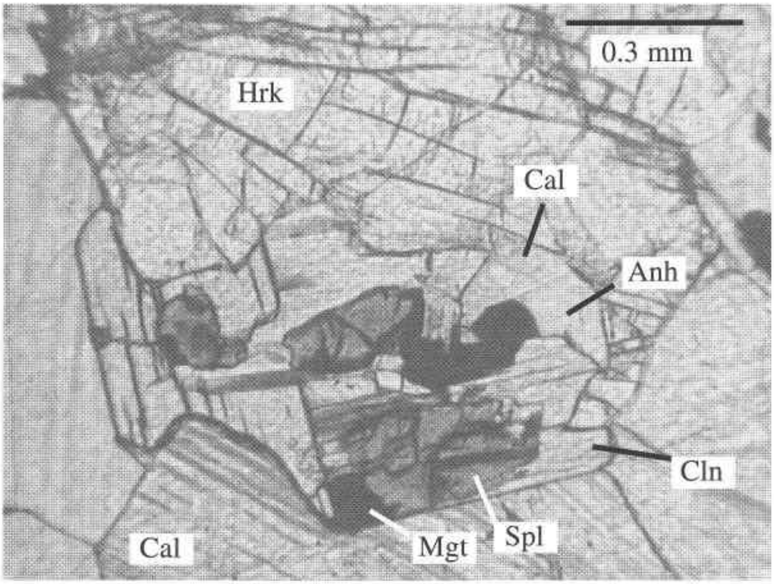

FIG. 4. Photomicrograph of harkerite (Hrk) and clintonite (Cln) aggregate with inclusions of spinel (Spl) in Crestmore marble #2A. Mgt: magnetite, Anh: anhydrite, Cal: calcite. Plane-polarized light.

TABLE 1. MINERALS IN MARBLE AND SKARN CONTAINING FRESH HARKERITE

	Crestmore quarry			Cascade Slide xenolith				Skye
	Marble	Marble	Skarn	Marble				Skarn
	1C	2A	3A	TM-16*	3	4	5	56016
Harkerite (Hrk)	x	x	x	1	x	x	t	x
Calcite (Cal)	x	x	x	62	x	x	x	x
Forsterite (Fo)	x	x	–	1	–	t	–	–
Monticellite (Mtc)	i	–	x	33	x	x	x	x
Clinopyroxene (Cpx)	–	–	–	2	i	–	x	t
Garnet (Grt)	–	–	–	–	t	–	t	t
Vesuvianite (Ves)	–	–	x	–	–	–	–	–
Clintonite (Cln)	x	x	x	–	–	–	–	–
Spinel (Spl)	i	x	x	1	t	x	–	–
Magnetite (Mgt)	t	t	–	–	t	t	–	–
Perovskite (Prv)	t	t	–	–	–	–	–	–
Pyrrhotite (Po)	t	–	–	–	t	–	–	–
Sphalerite	–	t	–	–	t	–	–	t
Cu–Fe sulfides	–	–	–	–	–	–	–	t
Anhydrite (Anh)	t	t	–	–	–	–	–	–
Barite	t	–	–	–	t	–	t	–
Apatite	–	t	–	–	–	–	–	–
Unknown Ca–Cl	–	–	–	–	–	–	–	t

Note: x: major constituent, t: trace constituent, i: occurs in trace amounts almost exclusively as inclusions in another phase. Abbreviations from Kretz (1983) and Grew (1996), except Mgt for magnetite. *Visual estimates from Baillieul (1976, Table 1).

that is characteristic of harkerite. On the basis of Baillieul's description and our finds, we suspect that harkerite is widespread in calcite marble at Cascade Slide.

Sections of specimens #1 and 2 contain no fresh harkerite, although fine-grained material characteristic of altered harkerite is present in #1. Clinopyroxene is abundant both as inclusions and as rounded inclusions in monticellite. In #1, garnet overgrows and embays clinopyroxene and forms microveinlets between calcite grains, whereas in #2, garnet is absent, its place being taken by clintonite, which embays clinopyroxene and encloses spinel.

Specimens #3, 4 and 5 (Table 1) consist dominantly of blue calcite in grains up to 1 cm across. Harkerite forms irregular masses with triangular projections into calcite and extending over 7 mm and locally enclosing monticellite (Fig. 5) or embaying it. Harkerite is birefringent (mostly first-order gray) and has fine polysynthetic twinning. The masses of harkerite are inferred to be aggregates of subhedral to euhedral octahedra; the twinning and anisotropy could have resulted from inversion to a non-isometric crystal system. Harkerite is commonly altered along fractures or in patches to very fine-grained material, in part rust-stained. Monticellite in rounded grains 1–4.5 mm across is the dominant silicate phase, whereas forsterite occurs only in #4 as partial overgrowths around monticellite. Some forsterite overgrowths widen and become poikilitic. Clinopyroxene is very pale yellow in thin section; it forms rounded inclusions in monticellite in #3, and equant grains 1–2.5 mm across in #5, where it is locally overgrown by monticellite or garnet. In #5, yellow garnet forms skeletal euhedral grains, overgrowths on clinopyroxene and

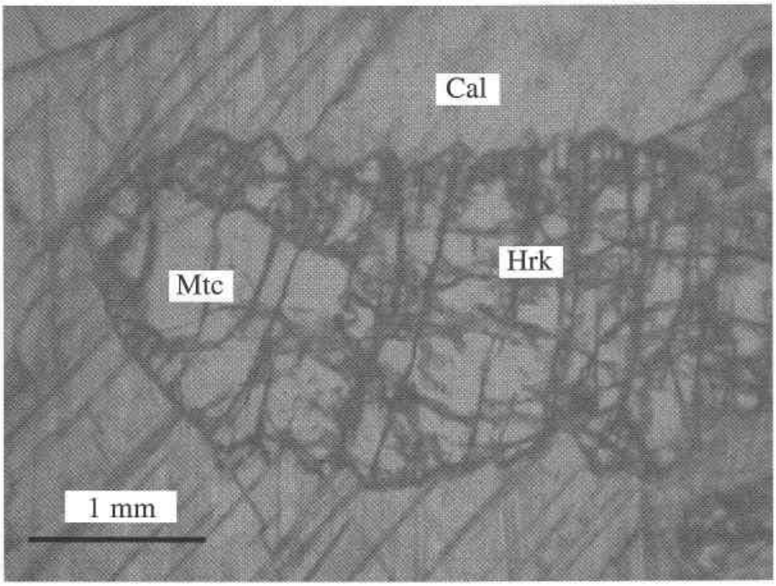

FIG. 5. Photomicrograph of harkerite (Hrk) with an inclusion of monticellite (Mtc) in Cascade Slide marble #4. Cal: calcite. Plane-polarized light.

inclusions in monticellite, whereas in #3, it forms overgrowths around spinel and monticellite. Green spinel forms rounded grains 0.05–0.35 mm across in calcite and monticellite; it is separated from harkerite by a garnet selvage. In #3, spinel is accompanied by tiny grains (*ca.* 0.05 mm across) of magnetite, whereas in #4, one grain of spinel is totally mantled by magnetite. Sphalerite and barite were recognized in back-scattered electron (BSE) images as inclusions in garnet and clinopyroxene, respectively; barite also is found near spinel.

Skye

A specimen of harkerite from the type locality, Skye (#56016, Harker Collection, University of Cambridge) was selected as an ion probe standard. This specimen consists of major monticellite and harkerite, minor andradite, sphalerite, and Cu–Fe sulfides; calcite, clinopyroxene, and an unidentified colorless phase are found in microveinlets (Table 1). Harkerite forms anhedral to euhedral (octahedral) grains typically 0.3–1 mm across. Patches of harkerite are weakly anisotropic and show very fine banding parallel to crystal faces in polarized light. Some grains have an atoll texture; in some cases, the core is riddled with fine inclusions, whereas in others, it is completely altered to a fine-grained material (mostly calcite?) that is separated from fresh material by a planar interface, which was illustrated by Tilley (1951). The clinopyroxene is close to end-member diopside (semiquantitative wavelength-dispersion analyses gave TiO_2 0.1, Fe as Fe_2O_3 0.8, Al_2O_3 0.5, MnO 0.4 wt%, Na_2O below detection), whereas the unknown contains only detectable Ca (~50% wt% CaO) and Cl. In other respects, the specimen corresponds closely to the material described by Tilley (1951), who also reported bornite, chalcocite, and magnetite.

X-RAY DIFFRACTION AND INFRARED DATA

X-ray powder-diffraction data (Debye–Scherrer camera) on harkerite in one sample of marble from underground at Crestmore (P. Adams, unpublished data using Ni-filtered Cu$K\alpha$ radiation) and in a sample from Cascade Slide [Baillieul (1976), using Mn-filtered Fe$K\alpha$ radiation] are in good agreement with data on harkerite from the type locality of Skye, U.K. (Tilley 1951, Ostrovskaya *et al.* 1966). All the lines with an estimated relative intensity greater than 5 and most of those with intensities of 4 or 5 (on a scale of 100) in the pattern reported by Ostrovskaya *et al.* (1966), and all lines of medium intensity and greater in Tilley's (1951) pattern, are present in the Crestmore and Cascade Slide patterns.

Harkerite from Crestmore #2A was analyzed by Fourier transform infrared (FTIR) spectroscopy from 4000 to 650 cm^{-1} using a Nicolet Magna 550 spectrometer equipped with a Nicplan microscope and an MCT–A detector. After a small amount of harkerite was crushed in a diamond compression cell, an area 100 μm in diameter of the crushed material was analyzed by transmission on one of the cell windows. The clean diamond window served as a background spectrum. The FTIR spectrum is virtually identical to those of the Skye harkerite and of a sample of harkerite of unknown provenance (Table 2, Fig. 6). The only major feature not

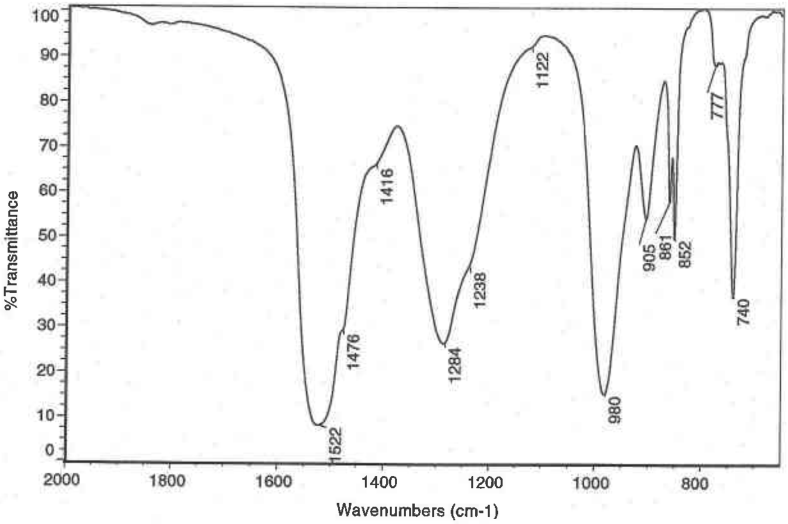

FIG. 6. FTIR spectrum of Crestmore harkerite (sample 2A).

TABLE 2. INFRARED SPECTRA OF HARKERITE*

1 Skye, U.K. cm^{-1}	2 Unknown cm^{-1}	3 Crestmore cm^{-1}	4 Assignment
1520	–	1522	CO_2
1510	1510	–	–
–	–	1476(s)	–
–	–	1416(s)	–
1300(s)	–	1284	BO_3
1245	1240	1238(s)	BO_3
–	–	1122(s)	SO_4(?)
975	980	980	SiO_4
910	912	906	SiO_4
865	865(d)	861	CO_2
855	855	852	CO_2
780	782	777(s)	BO_3
770	–	–	SiO_4
742	740	740	BO_3

* Over the range 700 to 1600 cm^{-1}. Sources: 1. Ostrovskaya *et al.* (1966), 2. Povarennykh & Nefedov (1971), 3. #2A, this paper. 4. Assignments are based on those made by Ostrovskaya *et al.* (1966) for harkerite and Ross (1974) for sakhaite. Note: s: shoulder, d: doublet.

matching features reported in the other spectra is at 1284 cm^{-1}; the shoulder at 1300 cm^{-1} (Ostrovskaya *et al.* 1966) is the closest. No feature at this position is reported in the spectra for sakhaite (Ostrovskaya *et al.* 1966, Povarennykh & Nefedov 1971). This absence could be due to the existence of only one B site in the sakhaite structure compared to two B sites in the harkerite structure (Giuseppetti *et al.* 1977). Variations in the relative heights of the 1245 cm^{-1} and 1284–1300 cm^{-1} features and in their positions could be due to variations in B content from one specimen of harkerite to another. For example, the spectra for Crestmore #2A and #3A differ in that two distinct features at 1230 and 1300 cm^{-1} are present in the spectrum of 3A, which contains less B than #2A (see below).

CHEMICAL COMPOSITION

Methods

Harkerite and associated minerals in three samples each from Cascade Slide and Crestmore, as well as in a specimen from the type locality (#56016), were analyzed for elements with $Z \geq 9$ with a wavelength-dispersion ARL SEMQ electron microprobe (EMP) at the University of Maine. The EMP was operated with a 15 kV accelerating voltage and 10 nA beam current; a $\phi(\rho z)$ correction scheme was used to reduce the data. The following standards were used for all the minerals except for Si, Al and Ca in clintonite: diopside (Si, Mg, Ca), rutile (Ti), corundum (Al), almandine (Fe), spessartine (Mn), orthoclase (K), jadeite (Na), scapolite (Cl), polylithionite (F), willemite (Zn), chromite (Cr) and barite (S). Clintonite was re-analyzed with kyanite (Si, Al) and wollastonite (Ca) as standards; this choice resulted in improved analytical totals. With rare exceptions, the content of each constituent given in the tables of compositions is an average of 10 analyses at a given spot, and one to three grains of each mineral were analyzed at one spot each in a given section. Unless the measured content of a given constituent exceeded the one-sigma standard deviation by more than 0.01 wt%, the constituent was considered to be at or below the limit of detection, and its content is given as zero in the tables of compositional data; for F, the cutoff was 0.03%.

The EMP data for harkerite were corrected for an estimated H_2O content of 0.6 wt% (corresponding to 4H per formula unit; *cf.* 0.81 wt%: Tilley 1951) and semiquantitative B_2O_3 and CO_2 contents from the ion-probe data.

The minerals were also analyzed for light elements with a Cameca ims 4f ion microprobe (secondary ion mass spectroscopy, SIMS) operated on the University of New Mexico (UNM) campus by a UNM – Sandia National Laboratories consortium. Harkerite was analyzed for B and C under the following operating conditions: $^{16}O^-$, nominal 10 kV primary acceleration voltage, beam current of 5 nA, 25 μm spot size, secondary beam voltage offset of 0 V, and an energy window of 25 V. Mass resolution of $M/\Delta M = 2500$ was sufficient to resolve the $^{12}C^+$ signal from the $^{24}Mg^{2+}$ signal. The ion signals of ^{11}B and ^{12}C were normalized to the ^{28}Si signal and SiO_2 (weight %).

It was originally hoped to obtain B and C contents in the harkerite from Cascade Slide and Crestmore from working curves scaled to the factors $(^{11}B/^{28}Si)*SiO_2$ and $(^{12}C/^{28}Si)*SiO_2$ in harkerite from the type locality (Skye). However, harkerite in specimen #56016 from Skye turned out to be compositionally heterogeneous. The analyzed points differ markedly in SiO_2, B_2O_3 and CO_2 (Table 3), even in an area of a few tens of μm across. Other standards for B at our disposal are Al-rich borosilicates that are unsuitable for harkerite because the very different matrix could have significant effects on ion yield. Consequently, we adopted a somewhat different approach to calibrate the B and C data. Normally, we use one set of values for SiO_2 (by electron-microprobe analysis, EMPA) and B_2O_3 (by wet chemistry or crystal-structure refinement) as input for each standard (*e.g.*, Grew *et al.* 1998). In the present case, the average result of the two published wet-chemical analyses for SiO_2, B_2O_3 and CO_2 (Tilley 1951, Ostrovskaya *et al.* 1966) were used. Two grains in #56016 were analyzed at six (1a–f) and four points (2a–d) with the SIMS, and at three points each (1a, 1bdf, 1ce, 2ad, 2b, 2c) with the EMP (Table 3). The EMPA points were selected to be as close as possible to the SIMS points. The average values of the ratios $^{11}B/^{28}Si$ and $^{12}C/^{28}Si$ for the 10 SIMS points were used to calculate a working curve. Not surprisingly, the average B_2O_3 and CO_2 contents of #56016 are close to the chemical data used as input (Table 3).

Because the average EMPA SiO_2 is close to the average result of the two wet-chemical analyses (Table 3),

TABLE 3. COMPOSITIONS OF HARKERITE FROM THE TYPE LOCALITY

Grain-point	SiO_2	B_2O_3	CO_2
		Wet chemical, bulk (wt.%)	
Tilley	14.17	7.77	14.94
Ostrovskaya *et al.*	12.74	9.20	13.90
Average*	13.46	8.49	14.42
	EMPA	SIMS†	SIMS†
56016-1a	13.30	9.25	13.65
56016-1b	12.33	8.59	13.81
56016-1d	12.33	8.55	13.47
56016-1f	12.33	8.67	14.07
56016-1c	13.25	7.73	14.45
56016-1e	13.25	8.26	14.79
56016-2a	14.90	8.90	13.55
56016-2d	14.90	8.20	15.32
56016-2b	13.23	8.90	14.37
56016-2c	14.26	7.01	15.72
Average 56016	13.55§	8.41	14.32
Standard Dev.‡	6.7%§	7.7%	5.4%

Note: * Average of the compositions reported by Tilley (1951) and Ostrovskaya *et al.* (1966). † Calculated from results of individual electron-microprobe analyses (EMPA) of SiO_2 and the working curve derived from the average $^{11}B/^{28}Si$ and $^{12}C/^{28}Si$ values and wet-chemical data. § Only the results of the six independent EMPA were averaged. ‡ Standard deviation (one sigma) is expressed as a percentage of the measured value.

using the average result of the wet-chemical determinations of B_2O_3 and CO_2 to calibrate the working curve is reasonable. For this reason, the B_2O_3 and CO_2 contents are given as "semiquantitative" in Table 4. In any case, differences in B_2O_3 and CO_2 contents between one analysis and another can be used to assess compositional variations whatever the accuracy associated with the absolute values.

Boron contents in the associated minerals were established under the same conditions used for Al-rich borosilicates (*e.g.*, Grew *et al.* 1998). The reported B contents could be systematically in error because of large differences in matrix between the unknowns (grossular – andradite, monticellite, forsterite, vesuvianite) and the ferromagnesian Al-rich borosilicates used as B standards. Nonetheless, the B contents measured in forsterite and monticellite are plausible because they are consistent with crystal-chemical considerations (see below). Clintonite was analyzed using muscovite as a standard for Li and B.

Harkerite

Interpretation of the chemical composition of harkerite is impossible without a brief review of its crystal chemistry (Giuseppetti *et al.* 1977) and that of the closely related mineral sakhaite, approximately $Ca_{48}Mg_{16}(BO_3)_{28}(CO_3)_{16}Cl_4(OH)_8(H_2O)_4$ (Ostrovskaya 1969, Chichagov *et al.* 1974, Yakubovich *et al.* 1978). The crystal structure of these two minerals is built up of BO_3 and CO_3 triangles, SiO_4 and AlO_4 tetrahedra, MgO_6 octahedra, and CaO_8 polyhedra. A distinctive feature is the tetrahedral pentamer $[Al(SiO_4)_4]^{-13}$ (*e.g.*, Dirken *et al.* 1995), which substitutes for four unpolymerized $(BO_3)^{-3}$ triangles in both harkerite and sakhaite (Machin & Miehe 1976). Ostrovskaya (1969) suggested that charge balance could be achieved by incorporation of Cl or H with the $[BO_3]_4^{-12}$ cluster or with CO_3-for-BO_3 substitution. The substitution $Cl^- + [BO_3]_4^{-12} = [Al(SiO_4)_4]^{-13}$ is consistent with chemical data on most harkerite, but is not viable if Cl is incorporated as HCl, as Giuseppetti *et al.* (1977) deduced. Charge balance is possible both locally (Giuseppetti *et al.* 1977) and globally if the pentamer composition is $[AlSi_4O_{15}(OH)]^{-12}$.

The structures of harkerite and sakhaite contain two large cages with diameters of roughly 3.4 Å and 6.4–6.5 Å. Chlorine (or HCl) is reported to occupy the larger cavity in harkerite; H_2O is reported in both minerals. Ostrovskaya *et al.* (1966) cited the presence of bands in the region of 2800–3000 cm^{-1} and near 3200 cm^{-1} of the infrared spectrum as evidence for strong H-bonds in

TABLE 4. SELECTED COMPOSITIONS OF HARKERITE

	Ideal	Skye		Crestmore			Cascade Slide	
Sample #	-	56016	56016	1C	2A	3A	3	4
Grain #	-	1bdf*	2ad*	1	2	1ab§	1	1
				Electron microprobe, wt%				
SiO_2	16.372	12.33	14.90	14.69	10.89	16.02	15.90	15.94
Al_2O_3	3.473	2.37	2.73	2.89	2.31	3.24	2.92	2.83
FeO	–	0.80	0.83	0.61	0.52	0.57	0.76	0.80
MgO	10.982	10.81	10.84	10.61	10.67	10.45	10.83	10.90
CaO	45.841	46.05	45.44	45.28	44.69	45.55	44.00	44.39
SO_3	–	0	0	0.09	0.23	0.08	0	0
Cl	1.207	1.41	1.14	1.32	2.35	1.25	1.24	1.25
				Ion microprobe (SIMS), semi-quantitative, wt%				
B_2O_3	9.485	8.60	8.55	5.92	9.55	6.38	5.87†	6.07
CO_2	11.992	13.78	14.44	13.52	15.62	14.66	14.95†	14.36
				Calculated, wt%				
H_2O	0.921	0.93	0.92	0.91	1.20	0.91	0.90	0.91
O≡Cl	-0.27	-0.32	-0.26	-0.30	-0.53	-0.28	-0.28	-0.29
Total	100.001	96.76	99.53	95.45	97.27	98.75	97.09	97.16
				Formulae normalized to Ca + Mg + Fe = 64				
Si	16.000	11.934	14.550	14.499	10.852	15.808	15.919	15.822
Al	4.000	2.704	3.142	3.362	2.713	3.768	3.446	3.311
Si +Al	20.000	14.638	17.692	17.861	13.565	19.576	19.365	19.133
B	16.000	14.368	14.412	10.086	16.427	10.867	10.145	10.400
C	16.000	18.209	19.251	18.218	21.251	19.750	20.435	19.459
Fe^{2+}	–	0.648	0.678	0.504	0.433	0.470	0.636	0.664
Mg	16.000	15.598	15.780	15.612	15.851	15.372	16.165	16.129
Ca	48.000	47.754	47.542	47.884	47.716	48.158	47.199	47.207
Sum	116.000	111.215	115.355	110.165	115.243	114.193	115.945	112.992
HCl	2.000	2.313	1.887	2.208	3.969	2.090	2.104	2.103
OH	4.000	4.000	4.000	4.000	4.000	4.000	4.000	4.000
S	–	0	0	0.067	0.172	0.059	0	0
X_{Fe}	–	0.040	0.041	0.031	0.027	0.030	0.038	0.040

Note: All Fe is expressed as Fe^{2+}. Zero: at or below detection limit, Dash: not analyzed or not calculated. Ideal formula is from Giuseppetti *et al.* (1977). $X_{Fe} = Fe/(Fe^{2+} + Mg)$. * Levels of TiO_2, Cr_2O_3, and ZnO determined at one point only. †Average result of two SIMS analyses. §Average result of two very similar EMPA and SIMS analyses. TiO_2, MnO, ZnO, K_2O, Na_2O, and F are at or below detection. Brief counting with the SIMS showed a trace of Li and little or no Be in harkerite from Skye and in #2 and #3 from Crestmore.

sakhaite, and Povarennykh & Nefedov (1971) reported infrared evidence for OH, but not H_2O, in harkerite.

We compare the observed compositions of harkerite to the ideal charged-balanced composition lacking molecular H_2O, $Ca_{48}\ Mg_{16}\ [AlSi_4\ O_{15}\ (OH)]_4\ (BO_3)_{16}\ (CO_3)_{16}\ (HCl)_2$ (Table 4). Harkerite formulae are normalized to Ca + Mg + Fe = 64 cations (Grew 1996) rather than to B + C + 0.8 (Si + Al) = 48 (Barbieri *et al.* 1977) because C contents deviate more from stoichiometry than Ca. The measured CaO and MgO + FeO contents approach the values in the ideal formula, except for a deficiency in Ca in the Cascade Slide harkerite. The light rare-earth elements (*LREE*) and Sr can substitute for Ca (Barbieri *et al.* 1977). The harkerite in Crestmore #1C and 2A, Cascade Slide #4 and Skye (#56016) was scanned with the EDS specifically for Sr, Y and the light rare-earths. Traces of La and Ce were found only in harkerite from Cascade Slide #4; we estimate that no more than a few tenths of a weight% oxide are present. No trace of Sr or Y was found, but the detection limit for Sr could be as high as 0.5 wt% SrO because of the interference between Si*K*α and Sr*L*α lines with the EDS. If the Sr content in the Cascade Slide harkerite exceeded 0.5 wt% SrO, which is equivalent to 0.3 *apfu* (atoms per formula unit) of Sr, there would be sufficient Sr to make up the Ca deficiency in these samples.

The maximum Si + Al contents in the Cascade Slide and Crestmore #3A harkerite (19.133-19.576 *apfu*) approach the ideal value of 20 *apfu*, which is theoretically the maximum possible. The theoretical maximum is obtainable in formulae normalized to Ca + Mg + Fe = 64 only if no Sr and rare-earth elements (*REE*) substitute for Ca. Aluminum increases regularly with Si, but in a ratio near 1:6 instead of the ideal 1:4 (Fig. 7). B varies inversely with Si + Al, resulting in a substitution approaching $(BO_3)_4 = Al_{0.75}\ Si_{4.25}\ O_{15.25}\ (OH)_{0.75}$ (Fig. 8). Boron contents are systematically lower than values

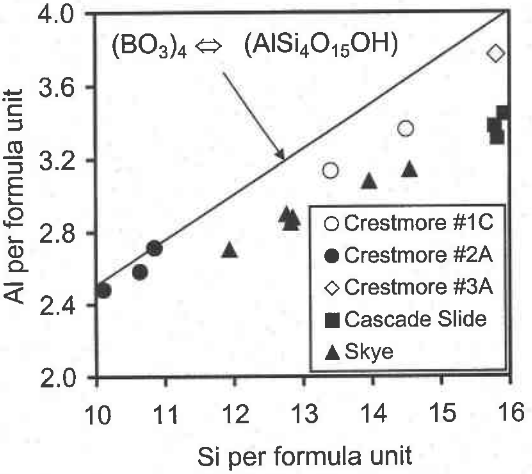

FIG. 7. Aluminum and silicon contents of harkerite. Line indicates ideal substitution.

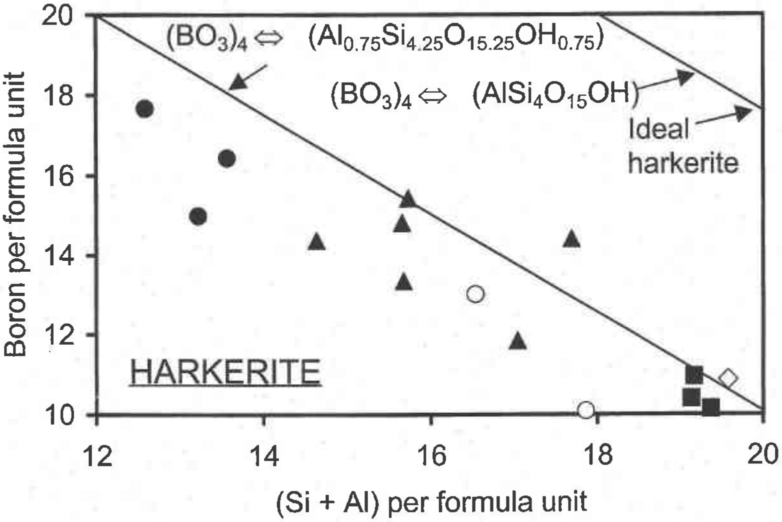

FIG. 8. Boron *versus* (Si + Al) content in harkerite. The line approximating the substitution in the analyzed samples is parallel to the line marked "ideal harkerite", which joins the ideal harkerite composition $Ca_{48}Mg_{16}[AlSi_4O_{15}(OH)]_4(BO_3)_{16}(CO_3)_{16}(H_2O,HCl)_2$ with an idealized sakhaite composition $Ca_{48}Mg_{16}(BO_3)_{32}(CO_3)_{16}(H_2O,HCl)_2$. The symbols identifying samples are the same as those in Figure 7.

predicted from the substitution $(BO_3)_4 = AlSi_4O_{15}(OH)$ operating on the ideal harkerite composition, whereas C contents exceed the ideal value of 16 *apfu*. Both features are characteristic of all analyzed samples of harkerite (*e.g.*, Giuseppetti *et al.* 1977, Barbieri *et al.* 1977). Substitution of BO_3 by 3OH (*e.g.*, Yakubovich *et al.* 1978) could make up the deficiency in B. Alternatively, the presence of calcite impurities in the standard analyzed in bulk by wet chemistry could result in B_2O_3 deficiency and CO_2 excess (*e.g.*, Giuseppetti *et al.* 1977), an error that would be propagated through the SIMS analytical results.

The wet-chemical (Tilley 1951, Ostrovskaya *et al.* 1966) and electron-microprobe data gave 2 Cl per formula unit in the Skye harkerite; Giuseppetti *et al.* (1977) inferred 50% occupancy equally divided between Cl and O on this site, *i.e.*, 1 Cl per formula unit. In the Crestmore and Cascade Slide material, B increases with Cl in a ratio of 3:1, close to the 4:1 ratio reported for harkerite overall (Grew 1996), but the Skye material lies off this trend (Fig. 9). The (Cl,O) site identified by Giuseppetti *et al.* (1977) can accommodate a maximum of 4 HCl if fully occupied and if H_2O is absent; in this way the ~4 Cl in Crestmore #2A can be accommodated. Possibly, the substitution proposed by Ostrovskaya (1969) can be written HCl + $[BO_3]_4^{-12} = [AlSi_4O_{15}(OH)]^{-12}$, where HCl is needed to fill the cage enclosed by the four BO_3 triangles rather than Cl^- for charge balance. In harkerite containing too little Cl to lie on the trend (*e.g.*, Skye, Fig. 9), H_2O could be filling the cage instead of HCl.

Harkerite from Crestmore contains a measurable amount of S (0.08–0.23 wt% SO_3), whereas S in harkerite from Cascade Slide and Skye is at or below detection limit. The S content is higher in samples containing anhydrite (1C, 2A) and negligible in the section containing the most sulfide (Skye), which suggests that S is incorporated in harkerite as sulfate and not as sulfide. The tiny shoulder at 1122 cm^{-1} in the FTIR spectrum of Crestmore #2A (Fig. 6) could be the main SO_4 absorption feature.

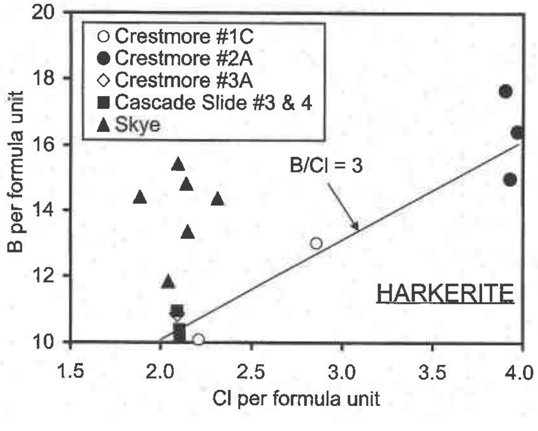

FIG. 9. Boron *versus* chlorine contents in harkerite. The line describes an ideal boron-to-chlorine ratio of 3:1. Cascade Slide #3 and 4 are plotted with the same symbol.

In calculation of the formula, Fe has been presumed to be Fe^{2+}. According to results of wet-chemical analyses, Fe^{2+}/Fe ranges from 0.38 to 1 in harkerite, and in most cases, exceeds 0.5 (*e.g.*, Tilley 1951, Ostrovskaya *et al.* 1966, Barbieri *et al.* 1977). Stoichiometry of the Crestmore and Skye harkerite suggests that most Fe could be Fe^{2+} replacing Mg, because Mg + Fe is approximately equal to 16 *apfu*. However, Mg in harkerite from Cascade Slide exceeds 16 *apfu*, and Al + Fe is approximately equal to 0.25 Si, the ideal value, which suggests that Fe^{3+} replacing Al is dominant. However, we suspect that Ca is less than 48 *apfu* in the harkerite from Cascade Slide (see above). If significant amounts of Sr or *REE* were replacing Ca and were not included in the formula normalization, then Mg would appear to exceed 16 *apfu*. In summary, it seems more reasonable to presume that Fe is mostly Fe^{2+} in all the samples of harkerite studied here.

The low analytical totals could be due to any one or all of the following: (1) underestimating B_2O_3 content because the measured B_2O_3 in the standard is too low, (2) unanalyzed Sr and rare-earth elements, and (3) H_2O contents well above 1 wt%, the amount equivalent to ~2 HCl and 4 OH per formula unit. Given the ambiguities in the anion occupancies and the absence of direct measurements of H_2O content, we have made no attempt to estimate the H_2O contents in the analyzed samples of harkerite beyond that inferred for ~2 HCl + 4 OH (~4 HCl + 4 OH in harkerite from Crestmore 2A). Although there is little evidence for H_2O in the larger cavities (Giuseppetti *et al.* 1977) or elsewhere in the harkerite structure (Povarennykh & Nefedov 1971), additional H_2O could be present as hydroxyl replacing BO_3 (Ostrovskaya 1969, Yakubovich *et al.* 1978).

Orthosilicates

Both monticellite and forsterite incorporate measurable amounts of B and F (Table 5). The amount of B in forsterite of Crestmore #2A is sufficient to show that it replaces Si (Fig. 10); in general, F content increases with B content; both features are characteristic of borian olivine from other localities (Sykes *et al.* 1994, Grew 1996).

In contrast, B contents of andradite – grossular from Cascade Slide and andradite from Skye are negligible (Table 6), which is characteristic of most examples of Ca-rich garnet (Grew 1996) except hydrogrossular – hydro-andradite from the Vilyuy River, Yakutia (Galuskin *et al.* 1995). Deficiency in Si is probably due to substitution by H and F: $\{\square\bullet(OH,F)_4\} \rightarrow \{SiO_4\}$; H_2O content has been calculated assuming that Ca + Mn + Mg + Fe + Ti + Al = 5 and Si + (F + OH)/4 = 3 (Valley

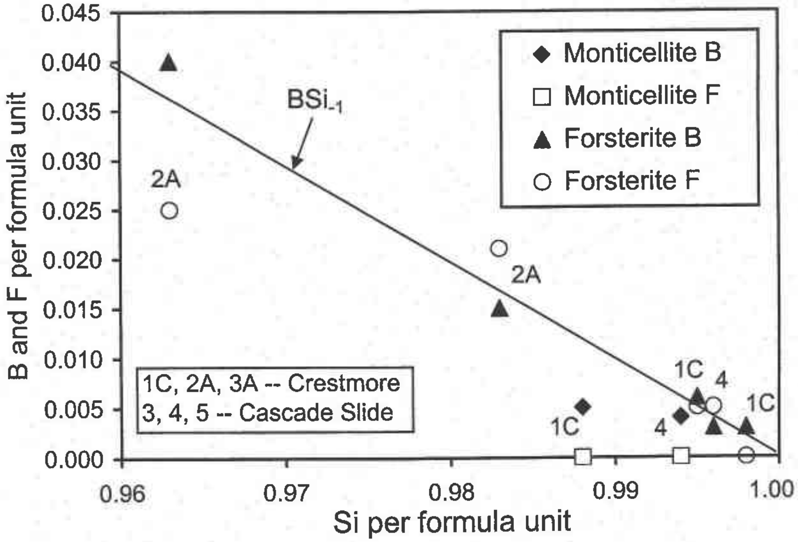

FIG. 10. Boron and F contents of monticellite and forsterite. The line describes an ideal B = Si substitution.

et al. 1983). Subsequent calculation of Fe^{3+}/Fe assuming total anionic charge of 24 gave a proportion of Fe^{3+} of 94% or more, *i.e.*, Fe^{2+} is essentially absent. Occupancies of the 8-coordinated and 6- coordinated sites approach the stoichiometric values of 3 and 2 cations, respectively, if Mg and Fe^{2+} are presumed to be octahedrally coordinated (Valley *et al.* 1983) rather than 8-coordinated as in pyrope – almandine solid solutions.

TABLE 5. SELECTED COMPOSITIONS OF MONTICELLITE AND FORSTERITE

	Skye	Crestmore					Cascade Slide	
	56016 Mtc	1C Mtc	1C Fo/1	2A Fo/1	2A Fo/2	3A Mtc	4 Mtc	4 Fo
	Electron microprobe, wt%							
SiO_2	37.33	37.68	42.03	41.57	41.04	37.94	37.48	41.88
FeO	4.33	2.70	2.53	2.05	1.90	2.88	4.51	2.70
MnO	1.06	0.16	0.17	0	0.11	0.32	0.42	0.39
MgO	21.81	24.50	54.76	55.74	56.31	23.27	22.89	54.64
CaO	35.50	35.46	0.30	0.23	0.24	35.41	34.85	0.19
ZnO	0.15	0	0	0	0	0	0	0
F	0.16	0	0	0.28	0.34	0	0	0
O≡F	-0.07	0	0	-0.12	-0.14	0	0	0
	Ion microprobe (SIMS), wt%							
B_2O_3	–	0.12	0.066	0.37	0.99	–	0.077	0.084
Total	100.27	100.62	99.86	100.12	100.79	99.82	100.23	99.88
	Formulae per 4 O							
Si	0.997	0.988	0.998	0.983	0.963	1.004	0.994	0.996
B	–	0.005	0.003	0.015	0.040	–	0.004	0.003
Fe^{2+}	0.097	0.059	0.050	0.041	0.037	0.064	0.100	0.054
Mn	0.024	0.004	0.003	0	0.002	0.007	0.009	0.008
Mg	0.868	0.957	1.939	1.965	1.969	0.918	0.905	1.937
Zn	0.003	0	0	0	0	0	0	0
Ca	1.015	0.996	0.008	0.006	0.006	1.004	0.991	0.005
Sum	3.004	3.009	3.001	3.010	3.017	2.997	3.003	3.003
F	0.013	0	0	0.021	0.025	0	0	0
X_{Fe}	0.101	0.058	0.025	0.020	0.018	0.065	0.100	0.027

Note: All Fe is expressed as Fe^{2+}. $X_{Fe} = Fe/(Fe^{2+} + Mg)$. Zero: at or below detection limit, Dash: not analyzed or not calculated. TiO_2, Al_2O_3, Cr_2O_3, Cl at or below limit of detection.

Deviations from stoichiometry in vesuvianite, *i.e.*, Si < 18 *apfu* of 50 cations and Ti + Al + Fe + Mg > 13 *apfu* (Table 6), are characteristic of boron-bearing vesuvianite, whereas the intermediate Al and Mg contents plot in the field of B-free vesuvianite (Groat *et al.* 1992, Fig. 15). Given that the Crestmore vesuvianite contains 767 ppm B, high Mg and low Al contents are not necessarily indicative of B-free vesuvianite.

Clinopyroxene

The clinopyroxene in Cascade Slide #5 is zoned (Table 7); the increase in Al in the rim is the reverse of the zoning reported by Tracy *et al.* (1978). A calculation of clinopyroxene composition assuming six atoms of oxygen and all Fe as Fe^{3+} results in cation totals exceeding four, implying little, if any, Fe^{2+} is present (Table 7), a conclusion also reached by Tracy *et al.* (1978) for clinopyroxene associated with forsterite ± monticellite in other specimens of marble from Cascade Slide.

Clintonite

The analyzed clintonite (Table 8) is comparable in composition to the more siliceous and least aluminous reported by Wiechmann (1995). Iron is presumed to be

TABLE 6. COMPOSITIONS OF GARNET AND VESUVIANITE

	Skye 56016 Grt	Cascade 3 Grt	Slide 5/1* Grt	xenolith 5/2** Grt	Crestmore 3A Ves
Electron-microprobe data, wt.%					
SiO_2	34.37	36.95	37.05	35.90	35.81
TiO_2	0	0.16	1.11	1.04	0.53
Al_2O_3	0.75	8.74	11.75	7.33	16.37
Fe_2O_3†	28.21	18.89	13.79	20.15	3.26
Fe_2O_3‡	28.21	18.89	13.45	19.43	–
FeO‡	0	0	0.31	0.65	–
MnO	0.18	0.09	0.13	0	0
MgO	0.70	0.25	0.80	0.38	4.02
CaO	33.72	34.86	35.22	34.46	36.65
F	0.14	0	0.12	0	0.24
Cl	0	0	0	0	0.09
O≡F, Cl	–0.06	0	–0.05	0	–0.12
Ion microprobe (SIMS), ppm					
B	6	1	1	1	767
Be	–	–	0	–	1
Calculated#					
H_2O	0.71	0.31	0.79	0.81	–
Total	98.72	100.25	100.68	100.00	96.85
Formulae calculated from cations and charge					
Cations		$\Sigma - Si = 5$			$\Sigma = 50^\$$
Charge§	23.869	23.982	24.000	24.000	–
Si	2.891	2.959	2.890	2.892	17.347
B	0	0	0	0	0.207
Ti	0	0.010	0.065	0.063	0.193
Al	0.074	0.825	1.080	0.696	9.346
Fe^{3+}	1.786	1.138	0.789	1.178	1.188
Fe^{2+}	0	0	0.020	0.044	–
Mg	0.088	0.030	0.093	0.046	2.903
Σ [6]	1.948	2.003	2.047	2.027	–
Mn	0.013	0.006	0.009	0	0
Ca	3.039	2.991	2.943	2.974	19.022
Σ [8]	3.052	2.997	2.952	2.974	–
Σ cations	7.891	7.959	7.889	7.893	50.206
OH#	0.397	0.164	0.411	0.433	–
F	0.037	0	0.030	0	0.368
Cl	0	0	0	0	0.074

Note: Zero – at or below detection limit, Dash – not analyzed or not calculated. Na_2O, K_2O, Cr_2O_3, and ZnO are at or below limit of detection. *Included in monticellite. **In calcite matrix. †Mesured. ‡Calculated. $Excluding B. §Anionic charge calculated from the cations. #From OH = 4(3-Si)-F, Valley et al. (1983).

all Fe^{3+} because previous wet- chemical and Mössbauer spectroscopic analyses of clintonite from Crestmore yielded Fe^{3+}/Fe values of 0.77–0.87 (Eakle 1916, Annersten & Olesch 1978).

Oxides

Calculation of spinel formulae assuming ideal stoichiometry yields $Fe^{3+} > Fe^{2+}$ in all cases (Table 9), a feature characteristic of other examples of spinel from Crestmore (Wiechmann 1995) and Cascade Slide (Baillieul 1976, Tracy *et al.* 1978, Valley & Essene 1980a). The magnetite – magnesioferrite solid solutions range in X_{Mg} [=Mg/(Mg + Fe) in molar proportions] from 0.32 to 0.64 and have low amounts of $MgAl_2O_4$–$FeAl_2O_4$ (Table 9, Fig. 11). Minor Ca was detected in most of the oxides, but magnetite #3A from Cascade Slide contains 0.63–1.15 wt% CaO. We infer that CaO measured in the oxides could result from fluorescence of Ca in calcite and monticellite surrounding the oxide grains, a problem that was particularly acute in the Cascade Slide #3A sample because the magnetite grains in this sample are smaller than the other oxide grains.

TABLE 7. RESULTS OF ELECTRON-MICROPROBE ANALYSES OF CLINOPYROXENE FROM CASCADE SLIDE*

	Core	Rim		Core	Rim
SiO_2 wt.%	50.81	50.09	Si *apfu*	1.847	1.825
TiO_2	0.37	0.36	$^{[4]}Al$	0.153	0.175
Al_2O_3	4.29	4.94	$^{[6]}Al$	0.031	0.037
Fe_2O_3	2.84	2.96	Ti	0.010	0.010
MnO	0.09	0	Fe^{3+}	0.078	0.081
MgO	16.08	15.95	Mn	0.003	0
CaO	26.21	26.20	Mg	0.871	0.867
			Ca	1.021	1.023
Total	100.69	100.50			
			Sum	4.014	4.018

The formulae are expressed in atoms per formula unit (*apfu*) on the basis of six atoms of oxygen. * Sample number 5. Note: All Fe is expressed as Fe^{3+}. Zero: at or below the limit of detection. Cr_2O_3, ZnO, K_2O, Na_2O, F, Cl at or below the limit of detection.

TABLE 8. COMPOSITIONS OF CLINTONITE FROM CRESTMORE

	1C	2A	3A		1C	2A	3A
Electron microprobe, wt%				Formulae per 22 atoms of oxygen			
SiO_2	17.11	17.03	16.52	Si *apfu*	2.419	2.419	2.340
TiO_2	0.10	0.07	0	$^{[4]}Al$	3.581	3.581	3.660
Al_2O_3	41.16	40.79	42.25	$^{[6]}Al$	3.277	3.247	3.393
Fe_2O_3	2.39	3.19	2.47	Ti	0.011	0.007	0
MgO	21.11	20.81	20.50	Fe^{3+}	0.254	0.341	0.263
CaO	13.35	13.06	13.29	Mg	4.449	4.406	4.329
F	0.07	0	0	Sum [6]	7.991	8.001	7.985
H_2O, calc.	4.21	4.22	4.23				
Total	99.47	99.17	99.26	Ca	2.022	1.987	2.017
				Sum Cat.	16.013	15.988	16.002
Ion microprobe (SIMS), ppm							
				OH	3.969	4.000	4.000
Li	-	-	3	F	0.031	0	0
B	-	-	2				

Note: All Fe is expressed as Fe^{3+}. Zero: at or below the limit of detection. MnO, ZnO, Cr_2O_3, K_2O, Na_2O, Cl at or below limit of detection.

TABLE 9. SELECTED RESULTS OF ELECTRON-MICROPROBE ANALYSES OF SPINEL-GROUP MINERALS

	Crestmore			Cascade Slide		Crestmore		Cascade Slide	
	1C	2A	3A	3A	4	1C	2A	3A	4
	–	1	–	1	2	2	2	1	1
	Spl	Spl	Spl	Spl	Spl	Mgt	Mfe	Mfe	Mgt
TiO_2	0.05	0.08	0	0.04	0.07	0.42	0.58	0	0
Al_2O_3	64.33	61.47	66.16	62.78	60.37	1.36	1.61	0.60	0.24
Cr_2O_3	0.18	0	0	0.07	0.09	0	0	0	0.07
Fe_2O_3	5.91	10.18	3.77	6.98	8.43	70.77	71.24	73.90	71.19
FeO	1.86	1.52	1.92	2.85	3.30	17.15	14.25	10.58	20.16
MnO	0.11	0.22	0.20	0.25	0.21	0.53	0.75	1.62	1.33
MgO	25.15	25.32	24.53	22.95	21.44	8.82	10.67	11.58	5.80
CaO	0.06	0.05	0	0	0.06	0.11	0.16	0.63	0.17
ZnO	1.45	1.24	2.80	3.93	5.31	0	0	0	0.19
Total	99.10	100.08	99.38	99.85	99.28	99.16*	99.26	98.91	99.15
				Formulae per 4 O and 3 cations (*apfu*)					
Ti	0.001	0.001	0	0.001	0.001	0.011	0.015	0	0
Al	1.884	1.806	1.930	1.865	1.832	0.058	0.067	0.025	0.010
Cr	0.004	0	0	0.001	0.002	0	0	0	0.002
Fe^{3+}	0.111	0.191	0.070	0.132	0.163	1.920	1.902	1.975	1.987
Fe^{2+}	0.039	0.032	0.040	0.060	0.071	0.517	0.423	0.314	0.625
Mn	0.002	0.005	0.004	0.005	0.005	0.016	0.023	0.049	0.042
Mg	0.932	0.941	0.905	0.862	0.823	0.474	0.563	0.613	0.321
Zn	0.027	0.023	0.051	0.073	0.101	0	0	0	0.005
Ca	0.002	0.001	0	0	0.002	0.004	0.006	0.024	0.007
Sum	3.000	3.000	3.000	3.000	3.000	3.000	3.000	3.000	3.000
X_{Fe}	0.040	0.033	0.042	0.065	0.079	0.522	0.429	0.339	0.661

The compositions are expressed as oxides, in wt.%. Note: The ratio Fe^{2+}/Fe^{3+} is calculated from stoichiometry. $X_{Fe} = Fe^{2+}/(Fe^{2+} + Mg)$. Zero: at or below the limit of detection. K_2O, Na_2O, F, Cl are below the limit of detection. Mfe: magnesioferrite. * Includes 0.06 wt% SiO_2, which was not used in the calculation of the formula.

TABLE 10. CONSTRAINTS ON OXYGEN FUGACITY AT 800°C

Buffering reaction	Limiting Oxygen fugacity
Wollastonite + magnetite + andradite[1]	near QFM (lower limit)
Orthopyroxene + olivine + magnetite[2]	HM + 2 log units (upper limit)
Anhydrite + magnetite + calcite + pyrrhotite[3]	near QFM

Note: HM: hematite + magnetite, QFM: quartz + fayalite + magnetite. Sources: 1: Gustafson (1974) and Liou (1974), 2: Johnston & Beckett (1986), 3: Estimated from Carroll & Rutherford (1987), Berman (1988) and Robie & Hemingway (1995) for log $a(CO_2)$ between –2 and –3.

Analyses of a perovskite grain in Crestmore #1C gave variable Ti (50.0–56.7 wt% TiO_2), relatively constant Ca (39.25% CaO) and Fe (1.21 wt% as FeO); totals are low (90.6–97.6 wt%). Scans of two grains with the EDS suggest that small amounts of U could be present, but no Th, W, Nb or Ta was found.

Compositional heterogeneity

Minerals in the harkerite-bearing rocks show overall compositional heterogeneity, but this is expressed more in terms of B, Si and Al than in Fe^{2+} and Mg. On the one hand, harkerite grains in the three Cascade Slide sections have similar SiO_2, B_2O_3, FeO, MgO and Cl contents (Figs. 7–9), and three grains in Crestmore #2A have similar Fe/Mg values. However, harkerite grains in both samples of Crestmore marble differ in SiO_2, B_2O_3, and CO_2; harkerite in #1C differ in Cl and Fe/Mg as well. Although the presence of zoning was not tested with the electron microprobe, there is no physical evidence of zoning in the Crestmore and Cascade Slide material, such as the atoll texture in the harkerite from Skye. There is no evidence for significant variation from grain to grain in Fe/Mg and Mn/Mg in monticellite. In forsterite, X_{Fe} [= Fe/(Mg + Fe)] varies somewhat from grain to grain, *i.e.*, X_{Fe} ranges from 0.021 to 0.025 in Crestmore 1C and from 0.018 to 0.020 in Crestmore 2A (Table 5). Variations in the B content of forsterite are more marked in Crestmore 2A. Garnet and clinopyroxene in Cascade Slide #5 are compositionally heterogeneous, *e.g.*, garnet enclosed in monticellite is notably richer in grossular than garnet in the calcite matrix (Table 6). In most cases, spinel and magnetite vary relatively little from grain to grain in Zn, Mn, Mg and calculated Fe^{3+} contents; an exception is the spinel of Cascade #3, in which Zn ranges from 3.93 to 5.28 wt% ZnO.

Element distribution

The distribution of Fe^{2+} and Mg between harkerite and associated forsterite, monticellite and spinel is regular (the Fe is presumed to be all Fe^{2+} in the orthosilicates:

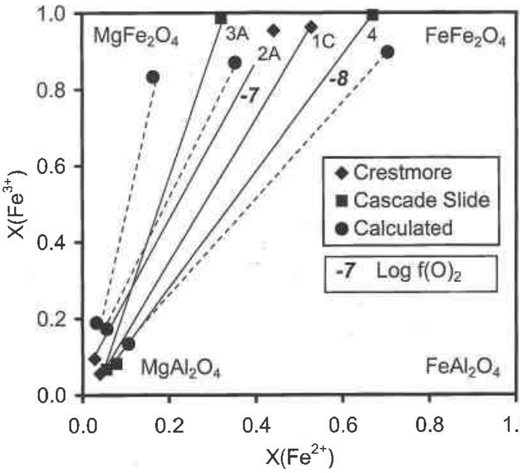

FIG. 11. Average compositions of coexisting spinel and magnetite plotted in the reciprocal system $MgFe_2O_4$–$FeFe_2O_4$–$MgAl_2O_4$–$FeAl_2O_4$. $X(Fe^{2+}) = Fe^{2+}/(Fe^{2+} + Mg)$; $X(Fe^{3+}) = Fe^{3+}/(Fe^{3+} + Al)$. Dashed lines indicate tie lines calculated by Lehmann & Roux (1986) for 800°C and 4 kbar. Log $f(O_2)$ values (italics) were estimated from Johnston & Beckett (1986, Fig. 4) using magnetite compositions, and represent the maximum possible for a given magnetite $X(Fe^{2+})$ because orthopyroxene is absent.

Fig. 12), which is consistent with Fe being largely ferrous in harkerite. However, the lines for harkerite – monticellite and harkerite – spinel intercept the abscissa at positive values of the ratio Fe^{2+}/Mg in harkerite, suggesting that minor Fe^{3+} could be present in harkerite. The line harkerite – forsterite intercepts the abscissa at a negative value of Fe^{2+}/Mg, which could result from the lack of documentation for more than three pairs.

Fe^{2+} is fractionated increasingly as follows: forsterite < harkerite < spinel < monticellite << magnetite. Increase of Fe^{2+}/Mg in magnetite with Fe^{2+}/Mg of associated orthosilicates is regular except for #3 from Cascade Slide. If iron in clinopyroxene and clintonite were considered to be all Fe^{2+} instead of Fe^{3+}, then their Fe^{2+}/Mg values would exceed the Fe^{2+}/Mg value of associated forsterite, a relationship contrary to that observed elsewhere (Obata *et al.* 1974, Ackermand *et al.* 1986).

Tie lines joining magnetite and spinel compositions form a regular array for three of the four samples (Fig. 11), which is consistent with equilibrium crystallization. The tie line for Cascade Slide 3A cuts across the others; the oxide compositions thus do not seem in equilibrium in this sample. Tie lines for the three equilibrated samples are also consistent with the array calculated for coexisting magnetite and spinel solid-solutions in the reciprocal system $MgFe_2O_4$–$FeFe_2O_4$–$MgAl_2O_4$–$FeAl_2O_4$ at 800°C and 4 kbar (Lehmann & Roux 1986). That is, Fe^{2+}/Mg distribution between the two oxides is consistent with crystallization at 800°C and has not been affected by retrograde or late, low- temperature redistribution that would have rotated the tie lines such that magnetite would have become more ferroan, and spinel more magnesian. However, the miscibility gap between magnetite – magnesioferrite and hercynite – spinel solid solutions is much wider than the solvus calculated by Lehmann & Roux (1986). In contrast, magnesioferrite reported from igneous rocks retain more spinel – hercynite in solid solution, *e.g.*, alkali gabbro from Hawaii (Johnston & Stout 1984). Thus it is possible that Fe^{3+} was lost from spinel – hercynite and Al from magnetite – magnesioferrite after crystallization. This readjustment apparently did not affect Fe^{2+}/Mg distribution.

INTERPRETATION OF THE MINERAL ASSEMBLAGES

Approach to chemical equilibrium is implied by (1) the regular distribution of Fe^{2+} and Mg among harkerite, forsterite, monticellite, spinel and magnetite, and (2) the reasonable compositional homogeneity with respect to Fe^{2+} and Mg. Consequently, it is possible to recognize the following stable mineral assemblages in the six samples:

harkerite + forsterite + clintonite + magnetite + calcite + anhydrite + pyrrhotite (Crestmore #1C marble)
harkerite + forsterite + clintonite + spinel + magnetite + calcite + anhydrite (Crestmore #2A marble)
harkerite + monticellite + clintonite + vesuvianite (+calcite?) (Crestmore #3A skarn)
harkerite + monticellite + spinel + calcite + pyrrhotite (Cascade Slide #3 marble)

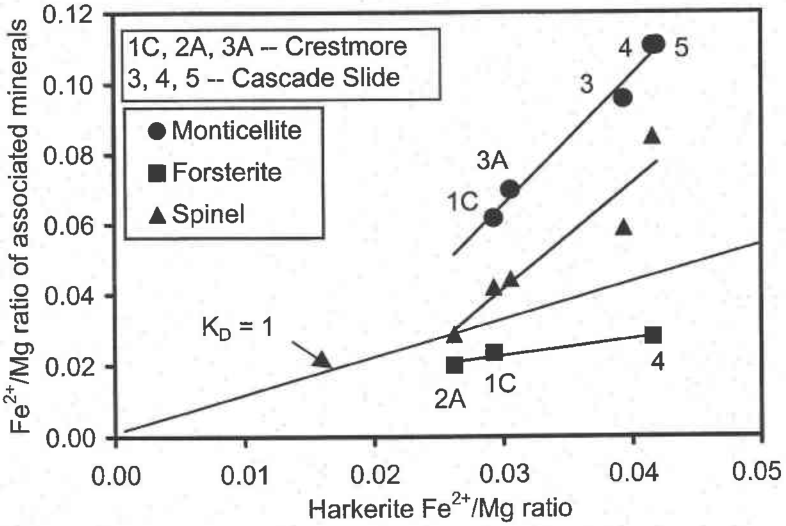

FIG. 12. Distribution of Fe^{2+} and Mg between harkerite and associated minerals. Lines are least-squares fits to the monticellite, spinel and forsterite data. Line marked $K_D = 1$ (= $(Fe^{2+}/Mg)_{other}/(Fe^{2+}/Mg)_{Hrk}$) represents an equal distribution of Fe^{2+} and Mg. Plotted values are average compositions for each mineral in a given sample.

harkerite + monticellite + forsterite + spinel + magnetite + calcite (Cascade Slide #4 marble)
harkerite + monticellite + clinopyroxene + calcite (Cascade Slide #5 marble).

Although textures imply that certain minerals crystallized after others, most of the minerals remained in contact, and by extension, equilibrated with one another. However, minerals apparently isolated from most of the others (spinel and monticellite in Crestmore #1C) and secondary minerals are not included in the assemblages. The position of a few minerals is ambiguous. Calcite is possibly secondary in Crestmore #3A. Textures of garnet suggest that it could be an early as well as a late phase in the Cascade Slide rocks, and thus it has not been included in the assemblages.

Sixteen components (CaO, MgO, FeO, MnO, ZnO, Fe_2O_3, Cr_2O_3, Al_2O_3, B_2O_3, TiO_2, SiO_2, H_2O, CO_2, SO_3, Cl, and F) are needed to fully describe the compositions of the minerals. Nonetheless, as a first approximation, the mineral assemblages can be projected through calcite, a ubiquitous phase, onto the (Mg, Fe)O–(Al, Fe)$_2$O$_3$–SiO_2 plane in order to assess the role of the components not projected (Fig. 13). Projection through CO_2 and H_2O, as well as CaO, allows for the possibility of external control of the fugacities of these two volatile components, a common practice in the portrayal of calcareous assemblages in contact aureoles (*e.g.*, Tracy & Frost 1991).

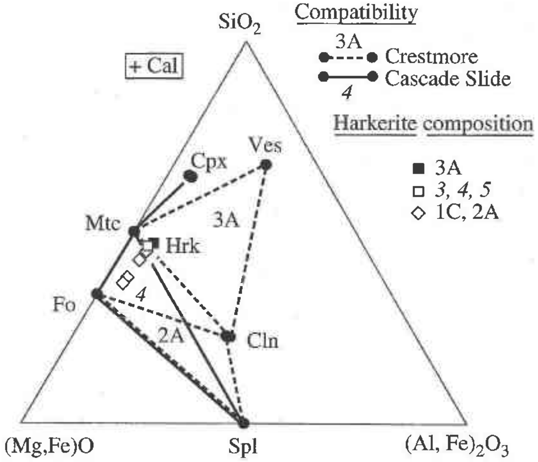

FIG. 13. Compositions of harkerite and associated minerals projected into the model system (Mg,Fe)O – (Al,Fe)$_2$O$_3$ – SiO_2 with calcite in excess, and CO_2 and H_2O presumed to be mobile components. The B and Cl contents of harkerite are ignored in this projection. Only three-phase assemblages are labeled. Mineral abbreviations are given in Table 1. Italics are used to distinguish Cascade Slide samples.

Figure 13 shows that the marble assemblages from Cascade Slide and Crestmore marbles are related by the following reaction calculated from simplified formulae:

4 Monticellite ($CaMgSiO_4$) + 3.6
Spinel ($MgAl_2O_4$) + 2 CO_2 + 2H_2O $\rightarrow$
1.6 Forsterite (Mg_2SiO_4) + Clintonite
[$Ca_2Mg_{4.4}Al_{7.2}Si_{2.4}O_{20}(OH)_4$] + 2 Calcite ($CaCO_3$)

Textures in Crestmore #1C suggest that the reaction did not quite proceed to completion in this particular sample. The presence of diopside + spinel in other samples of marble from Cascade Slide (Tracy *et al.* 1978, Valley & Essene 1980a) and apparent absence of clintonite + monticellite (these two minerals are not in direct contact in specimen #2, the only clintonite-bearing rock reported from Cascade Slide) place Cascade Slide on the high-temperature, high-$X(CO_2)$ side of the reaction:

0.36 Monticellite ($CaMgSiO_4$) + Clintonite
[$Ca_2Mg_{4.4}Al_{7.2}Si_{2.4}O_{20}(OH)_4$] + 0.91 CO_2 $\rightarrow$
1.45 Diopside ($CaMg_{0.9}Al_{0.2}Si_{1.9}O_6$) + 3.45 Spinel
($MgAl_2O_4$) + 0.91 Calcite ($CaCO_3$) + 2 H_2O

Although the two reactions imply that the spinel-bearing assemblages at Cascade Slide formed at higher temperature and $X(CO_2)$ than the Crestmore clintonite-bearing assemblages, the difference is more likely due to Zn, which is incorporated in spinel preferentially to other phases. Zn contents are as high as 11.3 wt% ZnO (0.20–0.22 Zn *apfu*) in the marbles containing diopside + spinel from Cascade Slide (Tracy *et al.* 1978, Valley & Essene 1980a), and thus could have stabilized monticellite + spinel and diopside + spinel at the expense of assemblages with clintonite.

Projection of harkerite compositions onto the plane (Mg, Fe)O–(Al, Fe)$_2$O$_3$–SiO_2 shows that its SiO_2 content reflects the mineral assemblage. The more siliceous compositions of harkerite are associated with monticellite (Crestmore #3A and all Cascade Slide sections), whereas the less siliceous compositions from Crestmore are associated with forsterite + clintonite ± spinel. (Fig. 13).

CONDITIONS OF FORMATION

Crestmore quarry

Crestmore is a classic metasomatic contact aureole in which SiO_2, Al_2O_3 and other oxides were introduced into a magnesian marble country-rock from tonalite and quartz monzonite at high temperatures and low pressures (*e.g.*, Burnham 1959). Wiechmann (1988, 1995) calculated peak temperatures of ~815 ± 15°C at 1.25 ± 0.25 kbar fluid pressure, and an $X(CO_2)$ of <0.010 during the first metasomatic event, when SiO_2 was introduced (*M*1). Wiechmann further reasoned that temperatures remained close to the peak during the second metasomatic event, when Al and subordinate Fe, Ti and Cr were introduced (*M*2). Typical *M*2 minerals are garnet, vesuvianite, gehlenite, clintonite, and spinel.

Harkerite is inferred to be a *M*2 mineral because it is found closely associated with spinel and clintonite. Thus, harkerite probably formed at T ≥ 800°C and P_{fluid} = 1.25 kbar. Anhydrite also appears to be coeval with clintonite and harkerite, and there is no reason to think that it is not also an *M*2 phase, although Wiechmann (1995) considered "wilkeite", which is sulfatian, silicatian apatite, a high-temperature (700°C or more) retrograde phase.

Boron minerals are found locally in the igneous and contact rocks at Crestmore (*e.g.*, Woodford *et al.* 1941, Burnham 1959), but have not been reported in unmetamorphosed limestone, and are rare in the metasomatized contact-rocks. It thus seems reasonable to assume that B originated in the igneous rocks and was introduced into the contact rocks. Situating harkerite as an *M*2 phase in Wiechmann's (1995) sequence implies introduction of B and Cl with Al during the second phase of metasomatism.

Cascade Slide xenolith

The Cascade Slide xenolith in the Marcy anorthosite massif has many features in common with Crestmore; indeed, the xenolith would appear to be another example of a classic high-temperature, low-pressure contact aureole, a similarity noted by previous investigators (*e.g.*, Tracy *et al.* 1978, Valley & Essene 1980a). Two minerals reported from Cascade Slide, monticellite and åkermanite, are characteristic of skarns formed in contact aureoles, but not of regional metamorphic terranes. However, the contact rocks at Cascade Slide developed in a very different geological context from Crestmore.

In contrast to the Crestmore marbles, B could have originated in the calcareous protolith at Cascade Slide and was not necessarily introduced from the anorthosite. Tourmaline is widespread in marbles of the Adirondack Highlands (Valley & Essene 1980b), and other boron-bearing minerals are found locally (Larsen & Schaller 1932, Grew *et al.* 1991).

The pressure–temperature conditions under which harkerite crystallized cannot be determined in a straightforward manner. The depth at which the Marcy anorthosite massif was emplaced and whether it was emplaced before a regional granulite-facies metamorphic event or coevally with this event are matters of debate. In general, the metamorphic rocks around the Marcy anorthosite massif appear to constitute a typical granulite-facies complex. Valley & Essene (1980a) calculated that the Cascade Slide åkermanite-bearing assemblage equilibrated at 750 ± 30°C, 7.4 ± 1 kbar, under granulite-facies conditions, which is consistent with other studies giving temperatures culminating at 780°C with P in the range 7–8 kbar for the Adirondack Highlands as a whole (*e.g.*, Bohlen *et al.* 1985, Kitchen & Valley 1995). Spear & Markussen (1997) estimated peak temperatures of ~800–850°C at P = 6.5–8 kbar for a large area of the Marcy anorthosite massif and its country rock, including Cascade Slide, whereas Alcock & Muller (in press) estimated temperatures of 850–950°C at pressures ~ 7.5 kbar for rocks in the contact of the Marcy anorthosite gneiss at Elizabethtown, about 20 km east–southeast of Cascade Slide.

Two scenarios have been proposed for the metamorphic evolution of the Adirondack Highlands. Valley & O'Neil (1982, 1984) and Whitney (1983) proposed a two-stage evolution: an early contact event in the aureole of the anorthosite emplaced at <3 kbar followed by granulite-facies metamorphism at depth. The $X(CO_2)$ for assemblages containing åkermanite, monticellite, or wollastonite is inferred to have been very low during the succeeding granulite-facies event (Valley & Essene 1980a, Valley *et al.* 1990, Valley & O'Neil 1982, 1984). Nonetheless, as emphasized by Valley *et al.* (1990), the low-pressure assemblages were not merely metastable relics, but did *equilibrate* under granulite-facies conditions. Thus, the distinctive assemblages in the Cascade Slide xenolith, including those with harkerite, crystallized at P < 3 kbar, but were stable following further burial because of the absence of a fluid phase. The alternative scenario is that the anorthosite was intruded at depth under granulite-facies conditions (*e.g.*, Wiener *et al.* 1984). Alcock & Muller (1999) cited evidence from near Elizabethtown, New York, that the anorthosite was emplaced at depths corresponding to 7.5 kbar and coeval with regional granulite-facies metamorphism. They estimated temperatures rising to 950°C or more at the contact with the anorthosite. According to this scenario, the mineral assemblages in the Cascade Slide xenolith formed at the granulite-facies pressure of 7.5 kbar, but at temperatures 150–200°C higher than the granulite-facies temperatures affecting rocks distant from the anorthosite contact.

Both scenarios require that the harkerite at Cascade Slide experienced pressures approaching 8 kbar. In addition, our chemical data are consistent with harkerite having been in chemical equilibrium with associated minerals at Cascade Slide as well as at Crestmore. Thus, harkerite can no longer be regarded as a typomorphic mineral of shallow intrusions and similar low-pressure environments ("sanidinite facies"); it is also stable at moderate pressures.

Oxygen fugacity

Wiechmann (1995) noted that fluids during the *M*2 event at Crestmore were oxidizing and became more so following *M*2, as evidenced, respectively, by the relatively high Fe^{3+} contents of spinel and by the high-temperature retrograde phase, SO_4-bearing apatite ("wilkeite"). The high Fe^{3+}/Fe value in clintonite reported by Eakle (1916) and Annersten & Olesch (1978) can also be cited as evidence for oxidizing conditions.

Tracy *et al.* (1978) cited the high proportion of Fe^{3+} in diopside as evidence that Cascade Slide marbles crystallized under oxidizing conditions. Another suggestion that conditions were relatively oxidizing is the relatively high $MgFe_2O_4$ content of magnetite (Frost & Lindsley 1991). Log $f(O_2)$ calculated from the magnesian magnetite compositions using the orthopyroxene + olivine + magnetite buffer of Johnston & Beckett (1986) range from –7 to –8 (Fig. 11). However, orthopyroxene is absent in the harkerite-bearing marbles, and consequently these calculated values are only an upper limit for a given composition of magnetite at 800°C. The absence of wollastonite gives a minimum possible $f(O_2)$ from the wollastonite + andradite + magnetite buffer (Table 10). The problem with this buffer is that among the magnetite-bearing rocks, andradite is present only in Cascade Slide #3, and there it is a secondary mineral.

Attempts to quantify the $f(O_2)$ during crystallization suggest intermediate oxygen fugacities near the quartz + fayalite + magnetite buffer, QFM (Table 10, Fig. 14). The pyrrhotite + anhydrite + magnetite assemblage in Crestmore #1C is a possible oxygen buffer:

calcite ($CaCO_3$) + pyrrhotite ($Fe_{0.9}S$) + 2.1 O_2 →
anhydrite ($CaSO_4$) + 0.3 magnetite ($FeFe_2O_4$) + CO_2

At a CO_2 activity reasonable for the marbles (0.001–0.01), the $f(O_2)$ buffered by the above reaction could be close to QFM. Crestmore #2A could be more oxidized than the buffer assemblage because pyrrhotite is absent, whereas the Cascade Slide marbles could be more reduced because anhydrite is absent and pyrrhotite is present in one sample. Increasing oxidation is correlated with decreasing Fe^{2+}/Mg in coexisting ferromagnesian minerals (Fig. 12), a relationship commonly observed in metamorphic rocks (*e.g.*, Chinner 1960) and further evidence for an approach to equilibrium.

CONCLUSIONS

The results of the present study have shown the following:

1. Variations in SiO_2, Al_2O_3 and B_2O_3 in harkerite approximately fit the substitution $(BO_3)_4 \rightleftharpoons Al_{0.75}Si_{4.25}O_{15.25}(OH)_{0.75}$. Relative to the idealized formula based on a crystal-structure refinement, harkerite contains excess CO_2 and is deficient in B, even if allowance is made for the above substitution. Overall, much remains to be explained about the crystal chemistry of harkerite, particularly the roles of SO_3, Cl (HCl), H_2O, and OH.

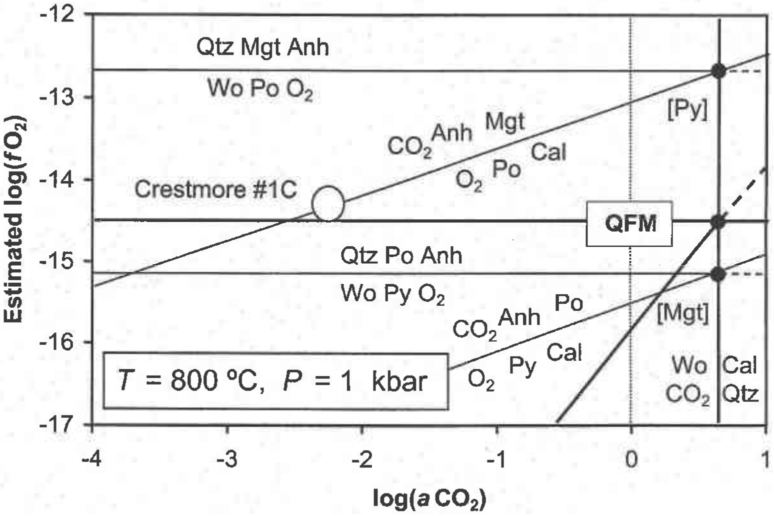

FIG. 14. Log $a(CO_2)$ – log $f(O_2)$ plot of reactions in the system Ca–Fe–Si–S–C–O relevant to an estimation of the oxygen fugacity conditions for the harkerite-bearing marbles. The area to the right of the dotted line [log $a(CO_2) > 0$] is inaccessible and is included only to complete the phase diagram. Abbreviations are given in Table 1 except Wo: wollastonite, Py: pyrite, Qtz: quartz, QFM: quartz + fayalite + magnetite; [ ]: encloses phase not involved in reaction at invariant point. Sources of data: Wo + CO_2 = Cal + Qtz (GE0–CALC, *e.g.*, Berman 1988); Qtz + Mgt + Anh = Wo + Po + O_2 (Carroll & Robinson 1987); QFM (Frost 1991). Locations of the other reactions were estimated from data of Robie & Hemingway (1995) and Berman (1987); these are only approximate. The positions of reactions involving magnetite apply only to the end-member composition [$a(FeFe_2O_4) = 1$]. The reaction 2 magnetite + 3 wollastonite + 3 CO_2 = O_2 + 3 fayalite + 3 calcite in the subsystem Ca–Fe–Si–C–O (heavy lines) is not labeled.

2. Forsterite, monticellite and vesuvianite associated with harkerite can incorporate some boron, whereas only traces of B were found in associated andradite – grossular and clintonite.

3. Harkerite crystallized in equilibrium with associated monticellite, forsterite, magnetite and spinel in marble and skarn from Crestmore and Cascade Slide. The distribution of Fe^{2+} and Mg is regular among these phases and varies systematically with estimated oxygen fugacity. Harkerite remained stable at pressures near 8 kbar at Cascade Slide. Near-absence of a fluid phase and low activities of CO_2, rather than low lithostatic pressure, are critical in stabilizing harkerite.

4. Despite the relatively high Fe^{3+}/Fe values of several phases, notably spinel and magnetite, oxygen fugacity estimated from the buffering assemblage anhydrite + magnetite + pyrrhotite + calcite is close to that for the QFM buffer. The "oxidized" compositions of spinel and magnetite could be a consequence of low Fe^{2+}/Mg and high temperatures. These conditions favor a more even distribution of Fe^{2+} and Mg between the two minerals, *i.e.*, increased $MgFe_2O_4$ content in magnetite, and a narrower solvus between spinel and magnetite solid-solutions, resulting in significant $(Mg,Fe)Fe_2O_4$ solid solution in spinel. Anhydrite (and other Ca-sulfate phases such as sulfatian apatite) and magnetite with significant magnesioferrite component could play an important role in determining the sulfur–oxygen budget in silica-undersaturated marbles metamorphosed to high temperatures.

ACKNOWLEDGEMENTS

The research was supported by NSF grant EAR95–26403 to the University of Maine. The ion-microprobe data presented here were measured at the University of New Mexico – Sandia National Laboratories SIMS facility, a national user facility supported in part by NSF grant numbers EAR 95–06611 and EAR97–06054. Steve Laurie of the Sedgwick Museum, University of Cambridge, is thanked for specimen #56016 of Skye harkerite from the Harker Collection. Charles Shearer is thanked for helping to obtain SIMS data on garnet and vesuvianite. We thank Eric Essene, John Valley, Mark Wiechmann and an anonymous reviewer for comments on earlier drafts.

REFERENCES

ACKERMAND, D., HERD, R.K. & WINDLEY, B.F. (1986): Clintonite of regional metamorphic origin, along the margin of the Fiskenaesset complex, West Greenland. *Neues Jahrb. Mineral., Abh.* **155**, 39-51.

ALCOCK, J. & MULLER, P. (1999): Very high-temperature, moderate-pressure metamorphism in the New Russia Gneiss Complex, northeastern Adirondack Highlands, metamorphic aureole to the Marcy Anorthosite. *Can. J. Earth Sci.* (in press).

ANNERSTEN, H. & OLESCH, M. (1978): Distribution of ferrous and ferric iron in clintonite and the Mössbauer characteristics of ferric iron in tetrahedral coordination. *Can. Mineral.* **16**, 199-203.

BAILLIEUL, T.A. (1976): The Cascade Slide: a mineralogical investigation of a calc-silicate body on Cascade Mountain, Town of Keene, Essex County, New York. *Univ. Massachusetts, Dep. Geol. Contrib.* **27**, 128 p.

BARBIERI, M., COZZUPOLI, D., FEDERICO, M., FORNASERI, M., MERLINO, S., ORLANDI, P. & TOLOMEO, L. (1977): Harkerite from Alban Hills, Italy. *Lithos* **10**, 133-141.

BERMAN, R.G. (1988): Internally-consistent thermodynamic data for minerals in the system $Na_2O–K_2O–CaO–MgO–FeO–Fe_2O_3–Al_2O_3–SiO_2–TiO_2–H_2O–CO_2$. *J. Petrol.* **29**, 445-522.

BOHLEN, S. R., VALLEY, J. W. & ESSENE, E. J. (1985): Metamorphism in the Adirondacks. I. Petrology, pressure and temperature. *J. Petrol.* **26**, 971-992.

BURNHAM, C.W. (1959): Contact metamorphism of magnesian limestones at Crestmore, California. *Geol. Soc. Am., Bull.* **70**, 879-920.

CARROLL, M.R. & RUTHERFORD, M.R. (1987): The stability of igneous anhydrite: experimental results and implications for sulfur behavior in the 1982 El Chichon trachyandesite and other evolved magmas. *J. Petrol.* **28**, 781-801.

CHICHAGOV, A.V., SIMONOV, M.A. & BELOV, N.V. (1974): Crystal structure of sakhaite $Ca_3Mg(BO_3)_2CO_3 \cdot xH_2O$. *Dokl. Akad. Nauk SSSR* **218**, 576-579 (in Russ.).

CHINNER, G.A. (1960): Pelitic gneisses with varying ferrous/ferric ratios from Glen Clova, Angus, Scotland. *J. Petrol.* **1**, 178-217.

DIRKEN, P.J., KENTGENS, A.P.M., NACHTEGAAL, G.H., VAN DER EERDEN, A.M.J. & JANSEN, J.B.J. (1995): Solid-state MAS NMR study of pentameric aluminosilicate groups with 180° intertetrahedral Al–O–Si angles in zunyite and harkerite. *Am. Mineral.* **80**, 39-45.

DUNN, P.J., PEACOR, D.R., NELEN, J.A., RAMIK, R.A. & INNES, J. (1990): A sakhaite-like mineral from the Kombat mine in Namibia. *Mineral. Mag.* **54**, 105-108.

EAKLE, A.S. (1916): Xanthophyllite in crystalline limestone. *J. Wash. Acad. Sci.* **6**, 332-335.

FROST, B.R. (1991): Introduction to oxygen fugacity and its petrologic importance. *In* Oxide Minerals: Petrologic and Magnetic Significance (D.H. Lindsley, ed.). *Rev. Mineral.* **25**, 1-9.

________ & LINDSLEY, D.H. (1991): Occurrence of iron-titanium oxides in igneous rocks. *In* Oxide Minerals:

Petrologic and Magnetic Significance (D.H. Lindsley, ed.). *Rev. Mineral.* **25**, 433-468.

Galuskin, E., Galuskina, I. & Winiarska, A. (1995): Epitaxy of achtarandite on grossular – the key to the problem of achtarandite. *Neues Jahrb. Mineral., Monatsh.*, 306-320.

Giuseppetti, G., Mazzi, F. & Tadini, C. (1977): The crystal structure of harkerite. *Am. Mineral.* **62**, 263-272.

Grew, E.S. (1996): Borosilicates (exclusive of tourmaline) and boron in rock-forming minerals in metamorphic environments. *In* Boron: Mineralogy, Petrology and Geochemistry (E.S. Grew & L.M. Anovitz, eds.). *Rev. Mineral.* **33**, 387-502.

________, McGee, J.J., Yates, M. G., Peacor, D.R., Rouse, R.C, Huijsmans, J.P.P., Shearer, C.K., Wiedenbeck, M., Thost, D. E. & Su, Shu-Chun (1998): Boralsilite, $Al_{16}B_6Si_2O_{37}$: a new mineral related to sillimanite from pegmatites in granulite-facies rocks. *Am. Mineral.* **83**, 638-651.

________, Yates, M.G., Swihart, G.H., Moore, P.B. & Marquez, N. (1991): The paragenesis of serendibite at Johnsburg, New York, USA: an example of boron enrichment in the granulite facies. *In* Progress in Metamorphic and Magmatic Petrology (L.L. Perchuk, ed.). Cambridge University Press, Cambridge, U.K. (247-285).

Groat, L.A., Hawthorne, F.C. & Ercit, T.C. (1992): The chemistry of vesuvianite. *Can. Mineral.* **30**, 19-48.

Gustafson, W.I. (1974): The stability of andradite, hedenbergite, and related minerals in the system Ca – Fe – Si – O – H. *J. Petrol.* **15**, 455-496.

Holtstam, D. & Langhof, J. (1995): Metamorphic harkerite from Nordmarks odalfält, Värmland, Sweden. *Geol. Fören. Stockholm Förh.* **117**, 151-152.

Innes, J. & Chaplin, R.C. (1986): Ore bodies of the Kombat mine, South West Africa/Namibia. *In* Mineral Deposits of Southern Africa (C.R. Anhaeusser & S. Maske, eds.). Geol. Soc. South Africa, Johannesburg, South Africa (1789-1805).

Johnston, A.D. & Beckett, J.R. (1986): Compositional variation of coexisting olivine, orthopyroxene and Fe/Mg-ferrite as a function of T and f_{O_2}: a geothermometer and oxygen-barometer. *Contrib. Mineral. Petrol.* **94**, 323-332.

________ & Stout, J.H. (1984): A highly oxidized ferrian salite-, kennedyite-, forsterite-, and rhönite-bearing alkali gabbro from Kauai, Hawaii and its mantle xenoliths. *Am. Mineral.* **69**, 57-68.

Kitchen, N. E. & Valley, J. W. (1995): Carbon isotope thermometry in marbles of the Adirondack Mountains, New York. *J. Metamorphic Geol.* **13**, 577-594.

Kretz, A. (1983): Symbols for rock-forming minerals. *Am. Mineral.* **68**, 277-279.

Larsen, E.S. & Schaller, W.T. (1932): Serendibite from Warren County, New York, and its paragenesis. *Am. Mineral.* **17**, 457-465.

Lehmann, J. & Roux, J. (1986): Experimental and theoretical study of $(Fe^{2+}, Mg)(Al, Fe^{3+})_2O_4$ spinels: activity–composition relationships, miscibility gaps, vacancy contents. *Geochim. Cosmochim. Acta* **50**, 1765-1783.

Liou, J.G. (1974): Stability relations of andradite–quartz in the system Ca–Fe–Si–O–H. *Am. Mineral.* **59**, 1016-1025.

Machin, M.P. & Miehe, G. (1976): $[Al(SiO_4)_4]^{13-}$ tetrahedral pentamers in harkerite. *Neues Jahrb. Mineral., Monatsh.*, 228-232.

Obata, M., Banno, S. & Mori, T. (1974): The iron–magnesium partitioning between naturally occurring coexisting olivine and Ca-rich clinopyroxene: an application of the simple mixture model to olivine solid solution. *Bull. Soc. Fr. Minéral. Cristallogr.* **97**, 101-107.

Ostrovskaya, I.V. (1969): The crystal structures of sakhaite and harkerite. *Trudy Mineral. Muzeya imeni A. Ye. Fersmana* **19**, 197-201 (in Russ.).

________, Pertsev, N.N. & Nikitina, I.B. (1966): Sakhaite – a new carbonatoborate of calcium and magnesium. *Zap. Vses. Mineral. Obshchest.* **95**(2), 193-202 (in Russ.).

Pertsev, N.N. (1965): Forsterite twins from magnesian skarns of Polar Yakutiya. *Trudy Mineral. Muzeya imeni A.Ye. Fersmana* **16**, 259-261 (in Russ.).

________ (1971): *The Parageneses of Boron Minerals in Magnesian Skarns.* Nauka, Moscow, Russia (in Russ.).

Povarennykh, A.S. & Nefedov, Ye.I. (1971): Infrared spectra of some beryllium and boron minerals. *Geol. Zh.* **31**(5), 13-27 (in Russ.).

Robie, R.A. & Hemingway, B.S. (1995): Thermodynamic properties of minerals and related substances at 298.15 K and 1 bar (10^5 pascals) pressure and at higher temperatures. *U.S. Geol. Surv., Bull.* **2131**.

Ross, S.D. (1974): Borates. *In* The Infrared Spectra of Minerals (V.C. Farmer, ed.). *Mineral. Soc., Monogr.* **4**, 205-226.

Spear, F.S. & Markussen, J.C. (1997): Mineral zoning, $P – T – X – M$ phase relations, and metamorphic evolution of some Adirondack granulites, New York. *J. Petrol.* **38**, 757-783.

Sykes, D., Rossman, G.R., Veblen, D.R. & Grew, E.S. (1994): Enhanced H and F incorporation in borian olivine. *Am. Mineral.* **79**, 904-908.

Tilley, C.E. (1951): The zoned contact-skarns of the Broadford area, Skye: a study of boron–fluorine metasomatism in dolomites. *Mineral. Mag.* **29**, 621-666.

Tracy, R.J. & Frost, B.R. (1991): Phase equilibria and thermobarometry of calcareous, ultramafic and mafic rocks, and iron formations. *In* Contact Metamorphism (D.M. Kerrick, ed.). *Rev. Mineral.* **26**, 207-289.

_______, JAFFE, H.W. & ROBINSON, P. (1978): Monticellite marble at Cascade Mountain, Adirondack Mountains, New York. *Am. Mineral.* **63**, 991-999.

VALLEY, J.W., BOHLEN, S.R., ESSENE, E.J. & LAMB, W. (1990): Metamorphism in the Adirondacks. II. The role of fluids. *J. Petrol.* **31**, 555-596.

_______ & ESSENE, E.J. (1980a): Akermanite in the Cascade Slide xenolith and its significance for regional metamorphism in the Adirondacks. *Contrib. Mineral. Petrol.* **74**, 143-152.

_______ & _______ (1980b): Calc-silicate reactions in Adirondack marbles: The role of fluids and solid solutions. *Geol. Soc. Am. Bull.* **91**, 114-117 (Part 1: Summary) and 720-815 (Part II).

_______, _______ & PEACOR, D.R. (1983): Fluorine-bearing garnets in Adirondack calc-silicates. *Am. Mineral.* **68**, 444-448.

_______ & O'NEIL, J.R. (1982): Oxygen isotope evidence for shallow emplacement of Adirondack anorthosite. *Nature* **300**, 497-500.

_______ & _______ (1984): Fluid heterogeneity during granulite facies metamorphism in the Adirondacks: stable isotope evidence. *Contrib. Mineral. Petrol.* **85**, 158-173.

WHITNEY, P. R. (1983): A three-stage model for the tectonic history of the Adirondack region, New York. *Northeastern Geol.* **5**, 61-72.

WIECHMANN, M.J. (1988): Mineral assemblage zoning in the Crestmore (California) contact metasomatic aureole. *Eos, Trans. Am. Geophys. Union* **69**(16), 514 (abstr.).

_______ (1995): *Contact Metamorphism and Skarn Formation at Crestmore, California.* Ph.D. thesis, Johns Hopkins Univ., Baltimore, Maryland.

WIENER, R.W., MCLELLAND, J.M., ISACHSEN, Y.W. & HALL, L.M. (1984): Stratigraphy and structural geology of the Adirondack Mountains, New York: review and synthesis. *In* The Grenville Event in the Appalachians and Related Topics (M.J. Bartholomew, ed.), *Geol. Soc. Am., Spec. Pap.* **194**, 1-55.

WOODFORD, A.O., CRIPPEN, R.A. & GARNER, K.B. (1941): Section across Commercial Quarry, Crestmore, California. *Am. Mineral.* **26**, 351-381.

YAKUBOVICH, O.V., YEGOROV-TISMENKO, YU.K., SIMONOV, M.A. & BELOV, N.V. (1978): The crystal structure of natural sakhaite $Ca_3Mg[BO_3]_2[CO_3]\cdot0.36\ H_2O$. *Sov. Phys. Crystallogr.* **23**, 225-226.

Received June 26, 1998, revised manuscript accepted November 15, 1998.